Cramér distance and discretizations of circle expanding maps II: simulations

Pierre-Antoine Guihéneuf, Maurizio Monge

CRAMÉR DISTANCE AND DISCRETIZATIONS OF CIRCLE EXPANDING MAPS II: SIMULATIONS

PIERRE-ANTOINE GUIHÉNEUF AND MAURIZIO MONGE

Abstract. This paper presents some numerical experiments in relation with the theoretical study of the ergodic short-term behaviour of discretizations of expanding maps done in [GM22].

Our aim is to identify the phenomena driving the evolution of the distance between the t-th iterate of Lebesgue measure by the dynamics f and the t-th iterate of the uniform measure on the grid of order N by the discretization on this grid. Based on numerical simulations we propose some conjectures on the effects of numerical truncation from the ergodic viewpoint.

Contents

1. Introduction

This article is the experimental part of a series of two papers aiming to understand the ergodic behaviour of discretizations of circle expanding maps (see [GM22]). By expanding map of the circle $\mathbf{S}^1 = \mathbf{R}/\mathbf{Z}$ we mean a C^r map $f : \mathbf{S}^1 \to \mathbf{S}^1$ $(r > 1)$ such that $f'(x) > 1$ for any $x \in \mathbf{S}^1$ (see Figure 1 for an example of such a map, described in Subsection 2.2). Note that these assumptions force the map to be of degree $d \geq 2$.

We identify the circle $\mathbf{S}^1 \simeq \mathbf{R}/\mathbf{Z}$ with its fundamental domain $[0, 1]$, and endow it with discretization grids, of parameter $N > 0$

$$E_N = \left\{ \frac{i}{N} \mid 0 \leq i < N \right\},$$

and discretization projections $P_N : \mathbf{S}^1 \to E_N$ defined by

$$P_N(x) = \frac{i}{N} \iff x \in \left[\frac{i - \frac{1}{2}}{N}, \frac{i + \frac{1}{2}}{N} \right).$$

This allow to define the *discretizations* $f_N : P_N \to P_N$ of the map f by $f_N = P_N \circ f|_{E_N}$. In other words, $f_N(x)$ is obtained from $f(x)$ by projecting on the closest point of the grid E_N. Of course, this models what happens when the computer iterates a map using a fixed number of digits — when $N = 2^k$, the set E_N represents the set of points with at most k binary places. We also set Leb_N the uniform probability measure on E_N.

Date: July 6, 2023.

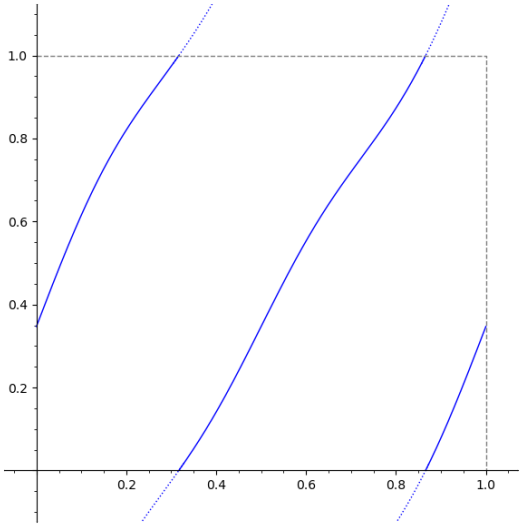

FIGURE 1. Graph of the studied expanding map (see Subsection 2.2).

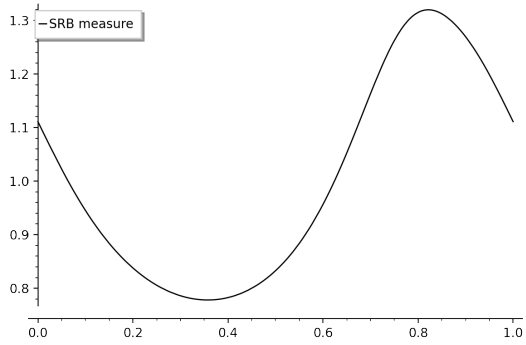

FIGURE 2. Density of the SRB measure associated to the map of Figure 1.

The basic example of expanding map $f : x \mapsto 2x$ shows that in some cases the discretizations dynamics does not reflect the chaotic properties of the map: if $N = 2^k$, then $f_N = f|_{E_N}$ and $f_N^k(x) = 0$ for any $x \in E_N$. In other words, any point of the grid is mapped after a small number of iterations on the fixed point 0: the dynamics of f_N is completely trivial.

To avoid these phenomena of resonance between the dynamics and the grid — that one can expect to be exceptional — one can consider *generic* dynamics. A property on expanding maps is said to be generic if it is satisfied on at least a countable intersection of open and dense subsets of the space of C^r expanding maps (for C^r topology). Baire's theorem ensures that a generic property is satisfied on a dense set of dynamics.

While some theoretical results are known about the *local* dynamics of discretizations of C^1 generic dynamics (*e.g.* [Gui15c]), *i.e.* the behaviour of individual discrete orbits, to our knowledge, the only known result about their *global* dynamics — that is, the properties taking into account, or averaging on, all points of the grid — deals with the *degree of recurrence* (see [Vla96] and [Gui19]). Besides this local/global dichotomy, one can classify the discretizations' dynamics into combinatorial and ergodic properties. Whereas combinatorial properties have been the subject of numerous numerical explorations, ergodic properties have been only little studied.

In this work (together with [GM22]), we intend to study the global ergodic behaviour of generic circle expanding maps discretizations.

The smoothness assumption on f ensures the existence of a unique absolutly continuous invariant measure, called SRB (for Sinai-Ruelle-Bowen), which is moreover ergodic, mixing and has the property that (and this is crucial here) the measures $f_*^k(\text{Leb})$ converge exponentially fast to it[1]. This measure is of great importance for the ergodic study of expanding maps, and its counterpart for higher dimensional hyperbolic maps opened the way to a whole branch of the ergodic theory. See Figure 2 for the graph of this measure's density in the case of the map of Figure 1.

[1]Meaning that the densities of these measures converge exponentially fast towards the density of SRB in the C^{r-1} topology

A large part of this paper will be devoted to the numerical comparison, for some expanding map f, of the actions of f and of its discretizations f_N on uniform measures. On the one hand, as said before, the iterates $f_*^k(\mathrm{Leb})$ converge exponentially fast towards SRB. On the other hand, what happens to the measures $(f_N^k)_*(\mathrm{Leb}_N)$, where Leb_N denotes the uniform measure on E_N, is much more unclear, especially as k grows together with N.

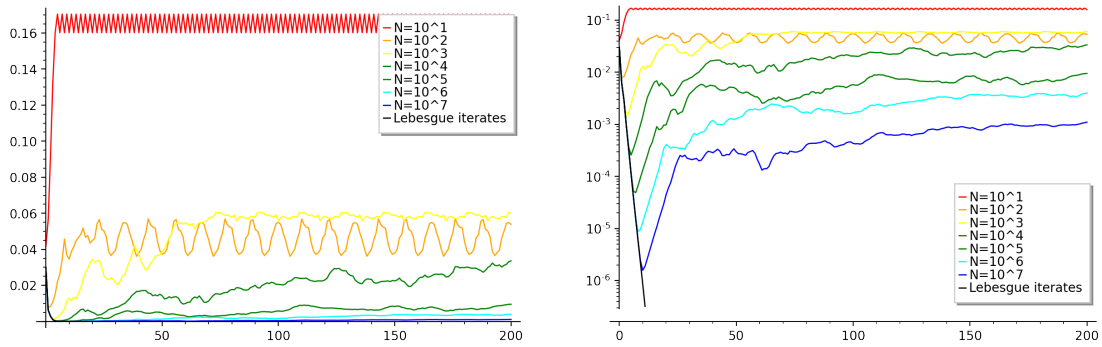

FIGURE 3. Graphs of $k \mapsto \mathrm{d_C}(f_*^k(\mathrm{Leb}), \mathrm{SRB})$ (black) and $k \mapsto \mathrm{d_C}((f_N)_*^k(\mathrm{Leb}_N), \mathrm{SRB})$ for various grid sizes N, uniform (left) and logarithmic (right) scales.

Figure 3 shows the evolution of $\mathrm{d_C}(f_*^k(\mathrm{Leb}), \mathrm{SRB})$ and $\mathrm{d_C}((f_N)_*^k(\mathrm{Leb}_N), \mathrm{SRB})$ with k, for different discretization orders N. Here, $\mathrm{d_C}$ is a distance on the set of probability measures, that we call *Cramér distance*, defined in Equation (2) page 8, and which spans the weak-* topology. This distance il also called Cramér-von Mises distance, or "the L_2-metrics between distribution functions" [Rac91, DM07].

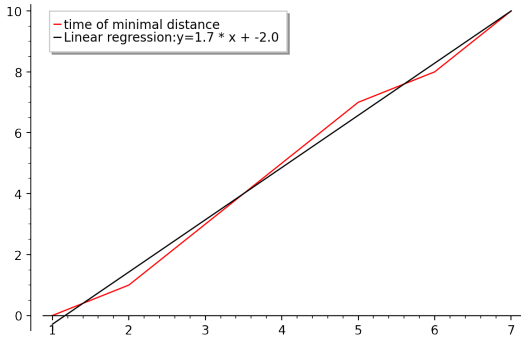

FIGURE 4. Argument of the minimum of the distance $k \mapsto \mathrm{d_C}((f_N)_*^k(\mathrm{Leb}_N), \mathrm{SRB})$ (*i.e.* time t_N for which this distance is minimal) depending on $\log_{10}(N)$, and linear regression of these values. This strongly suggests that this time t_N is of the order of $\log N$.

All the curves for the discretizations have more or less the same shape:

- They first decrease, up to a certain point, following quite well the corresponding curve for the actual dynamics f (in black), which decreases exponentially (see also Figure 5, left, for the plot of the densities of these measures). Figure 4 suggests a more or less linear relation between this time of minimum of the distance and $\log N$.
- Then they move away from the black curve and start to increase (see also Figure 5, right).

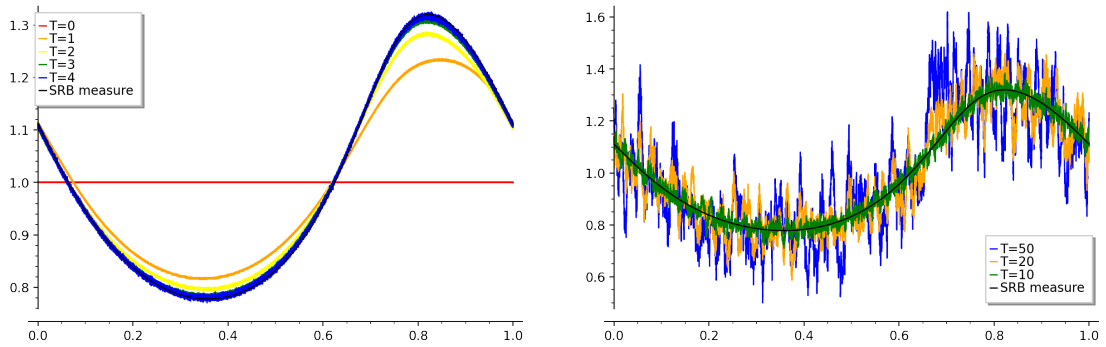

FIGURE 5. Densities of the measures $f_N^T(\mathrm{Leb}_N)$ for $N = 10^5$ and for different iteration times T, together with the density of the SRB measure. Note that as the measures $f_N^T(\mathrm{Leb}_N)$ are discrete, these measures are smoothed on intervals of size $500/N$ (*i.e.* they are convolved with the indicator function of these intervals).

- From a certain point, they seem to have a periodic behaviour (at least the ones for small values of the order N).

Let us explain the behaviour for small times. As a consequence of Theorem 2, for any $k \geq 0$, one has:

$$(f_N)_*^k(\mathrm{Leb}_N) \underset{N\to+\infty}{\longrightarrow} f_*^k(\mathrm{Leb}).$$

This is illustrated by Figure 5. See also [Gui15a, Theorem 12.17] for a proof with effective bounds on convergence speed. Roughly speaking, the operators $(f_N)_*$, acting on invariant measures, converge towards f_*. Hence, the behaviour of

$$k \mapsto \mathrm{d_C}\left((f_N)_*^k(\mathrm{Leb}_N), \mathrm{SRB}\right)$$

is the "combination" of the behaviours of

$$k \mapsto \mathrm{d_C}\left((f_N)_*^k(\mathrm{Leb}_N), f_*^k(\mathrm{Leb})\right) \qquad \text{and} \tag{1}$$

$$k \mapsto \mathrm{d_C}\left(f_*^k(\mathrm{Leb}), \mathrm{SRB}\right).$$

The second one is well understood, as $\mathrm{d_C}(f_*^k(\mathrm{Leb}), \mathrm{SRB})$ tends to 0 exponentially fast in k (combine Lemma 1 with the fact that the densities converge exponentially to the density of SRB in the C^{r-1} topology), so we are reduced to study the first map (1).

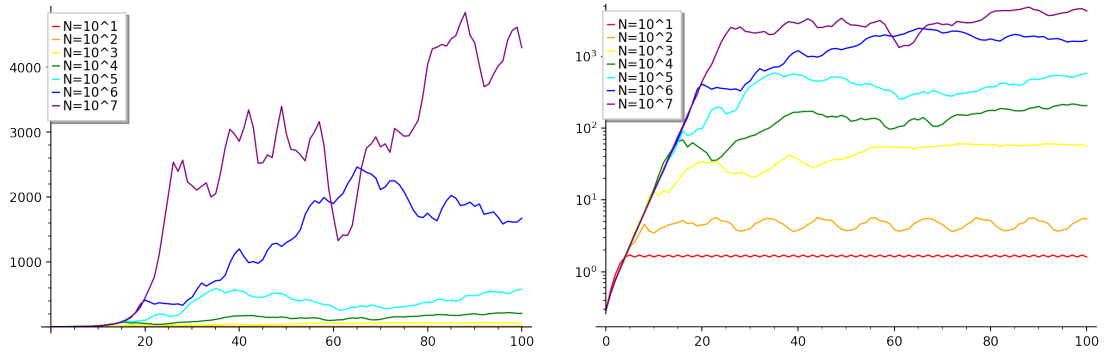

FIGURE 6. Graphs of $k \mapsto N\,\mathrm{d_C}((f_N)_*^k(\mathrm{Leb}_N), f_*^k(\mathrm{Leb}))$ for various grid sizes N, uniform (left) and logarithmic (right) scales. The factor N in front of the distance $\mathrm{d_C}$ is added so that the curves all start at $1/\sqrt{12}$ for the time $k = 0$ (the distance $\mathrm{d_C}$ between Lebesgue measure and the uniform measure on E_N is $1/(N\sqrt{12})$).

Figure 6 shows simulations of the first map (1). On these graphics there are three distinct time regimes:

- (R_1) The short-term behaviour, where the curves for discretizations seem to have a uniform behaviour: for a fixed time k and the grid parameter N going to infinity, they seem to converge to a curve that depends more or less exponentially on k (it is close to a line on the right graph which is in logarithmic scale). For this regime we have a theoretical prediction given by the asymptotics (5) of Theorem 2. We will confront this prediction with the actual simulations in the sequel.
- (R_2) The medium term behaviour, where the curve globally grows slowly.
- (R_3) The long-term or asymptotic behaviour, where the curve is periodic (at least for small values of N).

These three different regimes will guide our study of (1). More precisely, we will study these three regime separately and one after the other.

As proved independently in [DV98] and [Flo02], for a generic map of $\mathcal{D}^r(\mathbf{S}^1)$, the roundoff errors equidistribute: for a fixed time k, and the order N going to infinity, the sequence of roundoff errors in time k equidistributes in $[-1/(2N), 1/(2N)]^k$. See also [GM22, Proposition 3.2] for a more precise statement, which is obtained as a byproduct of the proofs.

So at first sight, one could expect the discretizations to behave very similarly to random perturbations. More precisely, the discretization f_N's global dynamics may be thought as the typical global dynamics of the random map f_t, acting on N-tuples of points of $\mathbf{S}^1$ such that each point x of this tuple is randomly drawn uniformly in $[f(x) - 1/(2N), f(x) + 1/(2N)]$.

In fact, things are a bit more subtle, and one quickly realizes that the fact that orbits of f_N can merge (*i.e.* that there exists distinct grid points that are eventually mapped to the same point under f_N) — and hence will stay together forever — must be an important parameter influencing the evolution of $(f_N)_*^k(\mathrm{Leb}_N)$. With this in mind, one can isolate (at least) four phenomena that make the action of discretizations different from that of a random map.

- (P_1) The iterates of points always belong to E_N.
- (P_2) Two points of E_N having the same image by f_N will have identical positive orbits.
- (P_3) The local shape around $y \in \mathbf{S}^1$ of the image $f_N(E_N)$ is very similar to the one of a linearization of f around the points $f^{-1}(y)$, which is a model set (see [GM22]).
- (P_4) Any point eventually falls in a periodic cycle.

Part of the paper will be devoted to the understanding of the relative effects of these phenomena on the action of discretizations on measures.

Conclusions. For each of the three different temporal regimes, we propose a model to describe it, accordingly to what numerical simulations suggest.

- The first one, (R_1), studied in Section 3, is the short term. It occurs for times $t \ll \log N$. In this regime, iterates of points that are initially microscopically close stay at a microscopical distance one from the others. The evolution of (1) is well described by Theorem 2 proved in the first paper of this series [GM22].
- The second one, (R_2), is the middle term, studied in Section 4. It seems to occur for times $\log N \ll t$ and $\log t \ll \log N$. In this regime, orbits of points that were neighbours at time 0 are typically at a macroscopic distance one from the other. Our simulations suggest that the main phenomena governing the evolution of (1) in this regime is (P_2): two points of the grid E_N having the same image by f_N will have identical positive orbits. On our simulations, the behaviour

of (1) looks a lot like the one of a random process described in Paragraph 4.2 (see (11)). This is a point process made of points with different weights, the local density of the points with weight $p \in \mathbf{N}$ being equal to the predicted local density of points with p preimages under the discretization f_N^t, this prediction being made by Proposition 6 (which reflects Phenomenon (P_2)). The expected Cramér distance $\mathrm{d_C}$ between the point process and the SRB measure is given by Theorem 9.

- The third one, (R_3), the long term, is studied in Section 5. It should happen for $\log t \gg \log N$ (or maybe $t \gg \sqrt{N}$, or $t \gg N$). What is the right model for this regime is more unclear than for the two other ones. It seems like that, as observed in the litterature (e.g. [Flo02, Lan98, ERDF83, Mie05, DKKP96, Bin92, Lev82]), the combinatorial behaviour is well described by the one of a random map on a set with N elements. Note that for some classes of interval maps having 0 as a fixed point, the combinatorial behaviour seem to be well described by a specific type of random maps called *random maps with a single attractive centre* [DKPV95, DSKP96]. Even if our simulations suggest that the asymptotic measures μ_N may converge towards SRB when N goes to $+\infty$, this conclusion is not so clear in view of phenomena such as rare orders N for which the measure μ_N is for away from SRB [Gui15b, Gui15a].

Some open problems. Of course, it is natural to ask whether such numerical phenomena hold in higher dimensions for systems with some hyperbolic properties (Anosov or Axiom A systems, systems with dominated splittings, etc.).

It is indeed a real challenge to tackle a theoretical validation of the numerical observations we outlined in this paper. As written by Lanford in [Lan98], "*[. . .] this problem may be as hard of that of non-equilibrium statistical mechanics.*"

We would like to put forward some research tracks that may be the first ones to address. First, one could try to get explicit times of convergence in Theorems 2 and 3 for some specific examples of piecewise real-analytic maps. Going a bit further, understanding why the first one is valid only in the short term and the second one remains true in the medium term would be an exceptional progress.

Also, adapting the proofs of [GM22] to the case of infinite branches circle expanding maps (e.g. Gauss map) may suggest other research directions. The program of previous paragraph may also be addressed in the case of the β-shift ($x \mapsto \beta x \mod 1$): the constant slope of the map may allow to undestand completely the discretizations' behaviours.

Bibliographical remarks. There are numerous numerical studies of the spatial discretization effects, but strangely only few works about these effects on ergodic properties.

A lot of these works focus on specific families of low-dimensional dynamics: [Bla98] for rotations and twist maps, [SB86] and [KMP99] for the tent map of slope ± 2, [Boy86] for a piecewise expanding map of slope ± 3, [DKP94] for $2x \mod 1$ (but for a random roundoff error model), [DKKP97, DKKP96, KMP99] for $1 - |1 - 2x|^\ell$, [Cor92, CFM90] for the Gauss map... These articles mainly focus on *combinatorial* properties of discretizations: such discretizations are finite maps, hence their combinatorial properties are roughly determined by the family of lenghts of periodic orbits and the size of their basins of attraction. This focus on combinatorial properties seems to have been initiated in [Lev82].

In [Lan98], after some illuminating general remarks, Lanford carries numerical simulations of the expanding map $x \mapsto 2x + x(1-x)/2$. Although mainly combinatorial,

one of them computes the measure carried by the longest detected cycle. On these simulations, these measures seem close to the SRB measure (the discretization is taken in the sense of the double precision).

More recently, Galatolo, Nisoli and Rojas [GNR14, Sections 6, 7 and 8] conducted numerical experiments on circle piecewise expanding maps (one example of which with a point with derivative 1) from an ergodic viewpoint. The difference with our study is that they consider Birkhoff averages of Dirac measures instead of the Lebesgue measure; their study is less extensive than ours but they still observe interesting behaviours of artefacts generated by roundoff errors. Their conclusion is that "*These experiments show that, in general, using floating point arithmetics to compute Birkhoff averages and invariant measures should not be considered reliable, not because of truncation and rounding errors, but rather because the dynamics of the discretised map does not mirror the generic dynamic of the real map.*"

There are few theoretical nontrivial results about the relations between discretizations and ergodic properties. In [GB88], Góra and Boyarsky get some theoretical results of convergence of the discretizations' asymptotic measures μ_N (see (12)) towards SRB, under the hypothesis that there exists large orbits for the discretization (of size $\geq \alpha N$ for a fixed $\alpha > 0$ and any N large enough). They check that this hypothesis holds for some piecewise linear maps of slope that are power of 3. However, [Gui19, Theorem 33] (see Theorem 3) shows that this hypothesis is not satisfied for generic dynamics... The two papers [Mie06] and [GS22] also focus on the effect of discretization on ergodic properties, in the case of circle homeomorphisms; these results emphasize some statistical stability of these particular systems under discretization.

In his PhD thesis [Flo02], Flockermann carries numerical simulations of maps which are similar to those considered in the present paper. However, these are mainly combinatorial: as in [Lan98], the only ergodic properties considered deal with the measure carried by some periodic orbits of the discretization. In this thesis the author also proves theoretical results about distribution of roundoff errors for generic circle expanding maps.

These results were obtained independently by Vladimirov in [Vla96] (further works based on this grounding article were published in [DV98, VKD00, DV02a, DV02b]). In this article, the author founds a solid theoretical basis about the discretizations' behaviour, which revals more powerful than Flockermann's approach: in addition to the equidistribution of roundoff errors, Vladimirov gets Theorem 3, and some functional central limit theorem, which was published with Vivaldi in [VV03]. Early apparitions of this kind of ideas can be found in the work of Voevodin [Voe67].

Part of these results were rediscovered independently (a second time!) by the first author in [Gui19]; this work also contains the case of diffeomorphisms and measure-preserving diffeomorphisms, it is based on an approach which, although a bit different, is quite similar to the one of [Vla96].

Acknowledgements. This project was partially supported by a PEPS/CNRS project and the ANR CODYS. The authors warmly thank Nina Heloin for his careful reading of a first version of this text, Djalil Chafai for the references about the name of our distance $\mathrm{d_C}$, and the anonymous referees for their very careful reading and unseful suggestions.

2. Preliminaries

2.1. **Distance on measures.** We will denote by $D^r(\mathbf{S}^1)$ the set of maps $f : \mathbf{S}^1 \to \mathbf{S}^1$ that are C^r and expanding (meaning that $f'(x) > 1$ for any $x \in \mathbf{S}^1$).

In the first paper of this series [GM22], we give an asymptotics of the distance between the measures $f_*^k(\mathrm{Leb})$ and $(f_N)_*^k(\mathrm{Leb})$, for k fixed and N going to infinity. This distance

is measured by what we call the *Cramér distance*: if μ and ν are two probability measures on $\mathbf{S}^1$, and F and G are their respective cumulative distribution functions defined from the starting point 0, we set $H = F - G$ and

$$\mathrm{d_C}(\mu,\nu) = \left(\min_{c\in\mathbf{R}} \int_0^1 (H-c)^2\right)^{1/2} = \left(\int_0^1 \left(H(x) - \left(\int_0^1 H\right)\right)^2 \mathrm{d}x\right)^{1/2}. \tag{2}$$

This is a distance spanning the weak-* topology on measures. For more details, see [GM22]. In particular, note that

$$\mathrm{d_C}(\mu,\nu)^2 = \mathbf{var}\big(H(\xi)\big) = \mathbf{E}\Big(\big(H(\xi) - \mathbf{E}H(\xi)\big)^2\Big),$$

where ξ is an auxiliary random variable with the uniform distribution on the unit interval $[0,1]$, and $\mathbf{E}(\cdot)$ is the expectation.

The following lemma is straightforward.

Lemma 1. *If μ and ν are two absolutely continuous probability measures on $\mathbf{S}^1$ with respective densities with respect to Lebesgue measure f and g, then*

$$\mathrm{d_C}(\mu,\nu) \le \|f-g\|_1 \le \|f-g\|_2 \le \|f-g\|_\infty.$$

Proof. In this case we have, for any $x \in [0,1]$,

$$F(x) = \int_0^x f(t)\,\mathrm{d}t$$

and the same for G, so

$$|H(x)| \le \int_0^1 |f-g|(t)\,\mathrm{d}t = \|f-g\|_1,$$

and

$$\mathrm{d_C}(\mu,\nu) \le \left(\int_0^1 H^2\right)^{1/2} \le \|f-g\|_1 \le \|f-g\|_2 \le \|f-g\|_\infty.$$

□

We will also use the *Ruelle-Perron-Frobenius* (RPF) operator, defined on observables $\phi : \mathbf{S}^1 \to \mathbf{C}$ by

$$L_f\phi : y \mapsto \sum_{f(x)=y} \frac{\phi(x)}{f'(x)}. \tag{3}$$

Note that if ϕ is the density of an absolutely continuous measure μ, then $L_f\phi$ is the density of $f_*\mu$. Here, the denominator in the definition of the RPF operator is $f'(x)$ instead of the classical modulus of the Jacobian determinant $|f'(x)|$ because f' is positive.

2.2. **The maps used in the simulations.** In our numerical studies, we will consider the following maps:

$$\begin{aligned} f_{c_1,c_2,k} : \mathbf{S}^1 &\longrightarrow \mathbf{S}^1 \\ x &\longmapsto 2x + c_1\sin(2\pi x) + c_2\sin(4\pi x) + k, \end{aligned} \tag{4}$$

with $c_1, c_2, k \in \mathbf{R}$ three parameters, with c_1, c_2 chosen such that the map f is expanding (which is true if $2\pi|c_1| + 4\pi|c_2| < 1$).

In most of the simulations, we will take $c_1 = c_1^0 = 0.0531647$, $c_2 = c_2^0 = 0.03932758$ and $k = 0.347$ (and in this case the minimum of $f'_{c_1,c_2,k}$ is bigger than 1.17). See Figure 1 for a graph of this map.

For some simulations, we will consider small perturbations of this system, by choosing $c_1 = c_1^0 + 0.001p_1$ and $c_2 = c_2^0 + 0.001p_2$, for

$$p_1, p_2 \in \left\{-1, -\frac{1}{2}, 0, \frac{1}{2}, 1\right\}.$$

2.3. **The code for the experiments.** The code we used for experiment is based on the *Python* project *CompInvMeas-Python* [MNP15] developed as an initiative to unify the approach to the computation of invariant measures explained in [GN14] using *SageMath* [The22], the framework and related further developments will be fully described in the article in preparation [GMNP23]. The code used from the project was forked from an older version and contains facilities to work with dynamical systems, to compute the Perron-Frobenius operator of an expanding dynamical system and to retrieve the corresponding numeric fixed point.

When the dynamics is expanding with a factor ≥ 2 it is possible to certify the error in the approximation of the SRB measure, estimating independently the numerical error which occurred while computing the numeric fixed point, and the mathematical error occurring representing the transfer operator with a finite-dimensional linear operator. While relevant, this estimation is very pessimistic therefore we used the result of the SRB measure in our experiments without adding the error coming from the rigorous error estimation, as it would have hidden the error coming from the spatial discretization.

Our experiments have been conducted in a notebook using the above facilities as a *Python* library, plus additionally a few support Python files offering facilities of our experiments. Such facilities are to compute different spatial discretizations of a dynamical system, to compute measure distances (Cramér and Wasserstein distance), and convenience functions to save intermediate results to a database in order to be able to interrupt experiments and resume them later. An end-to-end run of all the experiments takes several days and will create temporary files of roughly 500Gb.

The notebook with all the support file and the instructions to repeat the experiments is available on the url: `https://github.com/maurimo/DiscretizedDynSys`

3. Short term behaviour

3.1. **Theoretical result for Cramér distance.** In [GM22], we get an asymptotics for the map (1) for a generic expanding map.

Theorem 2 ([GM22])**.** *Let $r \geq 1$, f a generic C^r expanding map of the circle $\mathbf{S}^1$, and $k \in \mathbf{N}$. Then*

$$\lim_{N\to+\infty} N^2 \, \mathrm{d_C}\left((f_N^k)_*(\mathrm{Leb}_N),\, f_*^k(\mathrm{Leb})\right)^2 = \frac{1}{12} + \frac{1}{12}\sum_{m=0}^{k-1} \left\langle D(f^{k-m}), (L_f^m 1)^2 \right\rangle, \tag{5}$$

where $\langle \cdot, \cdot \rangle$ stands for the L^2 scalar product, L_f is the RPF transfer operator defined by (3), D is the derivative and f^{k-m} is the $(k-m)$-th iterate of f.

The aim of this section is to explore numerically the validity in practice of such results: the speed of convergence cannot be specified in the proof of Theorem 2 (it is hidden in the "generic" term).

As can be seen on Figure 7, the theoretical prediction is quite good up to time 20 for $N = 2^{23}$. More precisely, as can be seen on the left of Figure 8, the theoretical prediction stops being relevant from time $\simeq 18$. Note that for $N = 2^{23}$, one has $\log_2(N) = 23$; this behaviour of the time until when the theoretical prediction is accurate typically logarithmic in N is strongly suggested by Figure 8, right. In can be explained heuristically in the following way: for $N = 2^{23}$, as the derivative of the map f is everywhere close to

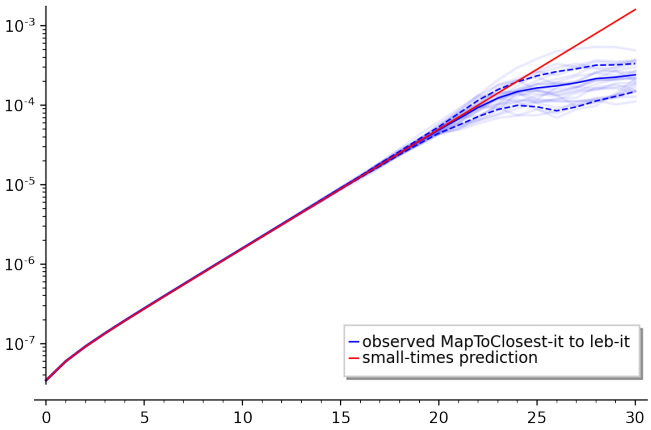

FIGURE 7. Distance (1) depending on time k, for $N = 2^{23}$, and for 25 perturbations of the map (4) described in Section 2.2 (in logarithmic vertical scale). The different curves for the different perturbations are in light blue, the blue curve represents the mean and the dashed curves the mean $\pm$ the standard deviation. The red curve is the theoretical prediction given by Theorem 2, and computed with the help of the RPF operator (3) for which we have a fast approximation algorithm.

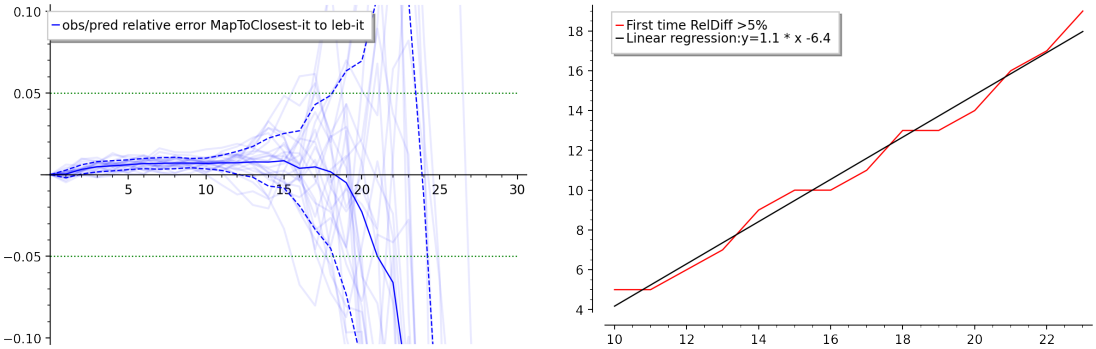

FIGURE 8. Left: relative difference between the theoretical prediction of Theorem 2 and the actual distances $\mathrm{d_C}$ on the examples for $N = 2^{23}$. Right: the x-axis represents $k = \log_2(N)$, the y-axis represents the first time for which the mean of the relative difference $\pm$ standard deviation is bigger than 5% (*i.e.* the first time one of the left blue dashed curves meets one of the green dotted lines) depending on $k = \log_2(N)$.

2, 20 is more or less the time needed for the iterations of a grid domain $[i/N, (i+1)/N]$ to become macroscopically visible.

Moral. In practice, Theorem 2 is valid until times logarithmic in N.

3.2. **Rate of injectivity.** Another quantity for which we have theoretical results is the *rate of injectivity*. It is defined as

$$\tau^k(f_N) = \frac{\mathrm{Card}\left((f_N)^k(E_N)\right)}{\mathrm{Card}(E_N)}.$$

This quantity (and the one studied in the next subsection) will be used in the study of the medium term behaviour of discretizations. In this subsection and the next one, we will:

- state theoretical results for these quantities, which will be proved for generic maps and small number of iterations;
- observe experimentally whether these theoretical results stay true in the short or medium term.

Before recalling the result of [Gui19], let us introduce some notations. Given an expanding map f of $\mathbf{S}^1$ of degree d, the set of time-k preimages of a point $y \in \mathbf{S}^1$ has a structure of complete d-ary tree, whose vertices are the points $x \in f^{-m}(y)$ for $0 \leq m \leq k$, and the edges are of the form $(x, f(x))$. One labels each edge $(x, f(x))$ of this tree by the number $1/f'(x)$, and denote by $T_k(y)$ the resulting labelled graph (see Figure 9).

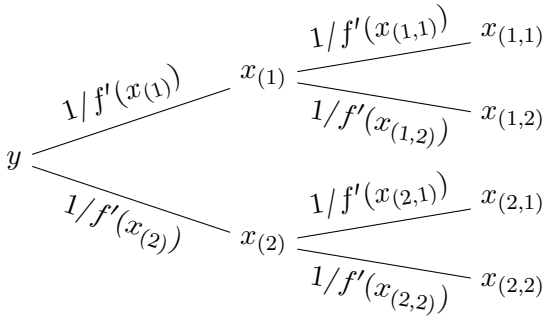

FIGURE 9. The probability tree $T_k(y)$ associated to the preimages of y, for $k = 2$ and $d = 2$. We have $f(x_{(1,1)}) = f(x_{(1,2)}) = x_{(1)}$, etc.

We call *random graph associated to f at y* the random subgraph $G_k(y)$ of $T_k(y)$, such that the laws of appearance of the edges $(x, f(x))$ in $G_k(y)$ are independent Bernoulli laws of parameter $1/f'(x)$. In other words, $G_k(y)$ is obtained from $T_k(y)$ by erasing independently each vertex of $T_k(y)$ with probability $1 - 1/f'(x)$.

We define the *mean density* $\overline{D}_k(y)$ as the probability that in $G_k(y)$, there is at least one path linking the root to a leaf.

The following is a restatement of [Gui19, Theorem 33] (see also [Vla96]).

Theorem 3. *Let $r \geq 1$, f a generic element of $\mathcal{D}^r(\mathbf{S}^1)$ and $k \in \mathbf{N}$. Then,*

$$\lim_{N \to +\infty} \tau^k(f_N) = \int_{\mathbf{S}^1} \overline{D}_k(y) \, \mathrm{d}\,\mathrm{Leb}(y). \tag{6}$$

As a byproduct of the proof of this theorem (and in particular Lemma 34 of [Gui19]), we get the following local convergence result (see also [Vla96]).

Proposition 4. *For any $r \geq 1$, for a generic expanding map $f \in \mathcal{D}^r(\mathbf{S}^1)$ and for almost every point y, one has*

$$\overline{D}_k(y) = \lim_{\substack{N,R \to +\infty \\ R/N \to 0}} \frac{1}{2R} \,\mathrm{Card}\left\{ \frac{i}{N} \in [y - R/N, y + R/N] \;\middle|\; \frac{i}{N} \in f_N^k(E_N) \right\}.$$

Note that a first step towards the proof of this theorem was realized in the unpublished thesis [Flo02].

The idea behind this theorem is the following. Assume for simplicity that $d = 2$, take some point $y \in \mathbf{S}^1$, and denote its preimages by f by x_0 and x_1. Then, in the neighbourhood of y, the set $f_N(E_N)$ looks like the discretization[2] of the set $f'(x_0)\mathbf{Z} \cup$

[2]Here, "discretization" stands for the projection on the nearest element of $\mathbf{Z}$, *i.e.* the image under the projection $\mathbf{R} \to \mathbf{Z}$ on the nearest integer.

$f'(x_1)\mathbf{Z}$. But, still in the neighbourhood of y, the "probability" for a point $z \in E_N$ to be in the discretization of the set $f'(x_0)\mathbf{Z}$ is equal to $1/f'(x_0)$. One of the steps in the proof of Theorem 3 is to show that the probabilities coming from the different branches are independent: the probabilities for a point $z \in E_N$ to be in the discretizations of the sets $f'(x_i)\mathbf{Z}$ are independent.

The following lemma gives a practical way to compute the percolation probability $\overline{D}_k(y)$, in terms of the transfer operator L_f associated to f (for which we have a fast and reliable algorithm).

Lemma 5. *For any $y \in \mathbf{S}^1$,*

$$\overline{D}_{k+1}(y) = 1 - \prod_{x \in f^{-1}(y)} \left(1 - \frac{\overline{D}_k(x)}{f'(x)}\right).$$

In particular, if the degree of f satisfies $d = 2$, denoting $f^{-1}(y) = \{x_0, x_1\}$, one has

$$\begin{aligned}\overline{D}_{k+1}(y) &= \frac{\overline{D}_k(x_0)}{f'(x_0)} + \frac{\overline{D}_k(x_1)}{f'(x_1)} - \frac{\overline{D}_k(x_0)\overline{D}_k(x_1)}{f'(x_0)f'(x_1)} \\ &= L_f(\overline{D}_k) - \frac{1}{2}\left(\left(L_f(\overline{D}_k)\right)^2 - L_f\left(\overline{D}_k^2/f'\right)\right).\end{aligned}$$

It is possible to get similar formulae for bigger d by using Vieta's formulas.

Proof. The first formula comes directly from the definition. The second one is a simple computation. □

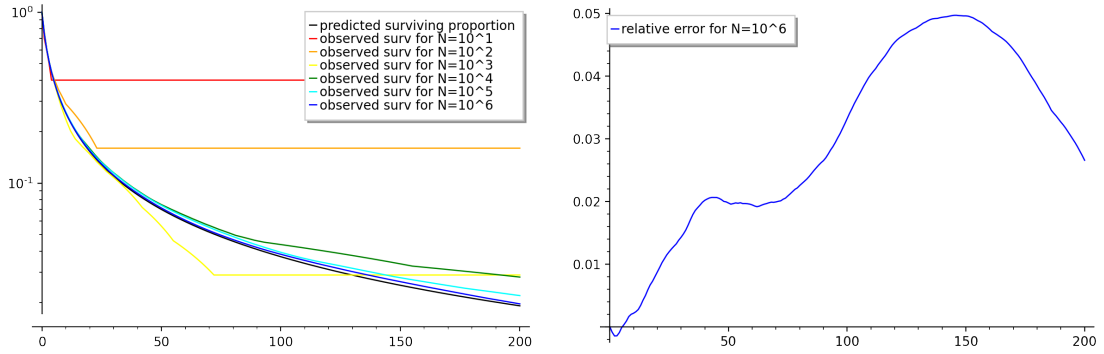

FIGURE 10. Left: rate of injectivity of $\tau^k(f_N)$ (the coloured curves) depending on k, for 6 different values of N: $10^1, 10^2, 10^3, 10^4, 10^5$ and 10^6. We also represent the theoretical value (given by Theorem 3, black curve) depending on k in logaritmic scale. Right: relative difference between these two quantities depending on k, for the biggest N ($N = 10^6$).

Figure 10 compares the theoretical rate of injectivity (the one given by Theorem 3 and computed with the help of Lemma 5) with the actual rate of injectivity of a discretization f_N, depending on the time k.

Moral. The predictions of Theorem 3 are really good during a quite long time (less than 5% up to time 200).

This contrasts with what happens for predictions of Theorem 2 (see Figure 7), that become inaccurate in times typically logarithmic in N. We do not have any clue why these predictions stay accurate for such a long time.

3.3. **Local distribution of preimages.** We pursue the study of the rate of injectivity by focusing on more precise quantities. We will look at the *distribution* of the number of preimages of a point of the grid. To do that, we set a_m (which depends on the point y and the time k) the probability that in $G_k(y)$, there are exactly m paths linking the root with the leaves. Denote by

$$\overline{P}_k(y) = \sum_{m \geq 0} a_m X^m \tag{7}$$

the associated generating series.

Of course, the polynomial $\overline{P}_k(y)$ is of degree at most d^k and satisfies $\overline{P}_k(y)(1) = 1$ and $\overline{P}_k(y)(0) = 1 - \overline{D}_k(y)$.

The proof of Theorem 3 links the limiting behaviour, for $N \to +\infty$, of the number of preimages of points of the grid E_N, with the random behaviour of the tree $G_k(y)$. Hence, as a byproduct of this proof, one gets the following result (see also [Vla96]).

Proposition 6. *For any $r \geq 1$, for a generic expanding map $f \in \mathcal{D}^r(\mathbf{S}^1)$ and for almost every point y, one has*

$$a_m = \lim_{\substack{N,R \to +\infty \\ R/N \to 0}} \frac{1}{2R} \operatorname{Card} \left\{ i/N \in [y - R/N, y + R/N] \;\middle|\; \operatorname{Card}\left(f_N^{-k}(i/N)\right) = m \right\}.$$

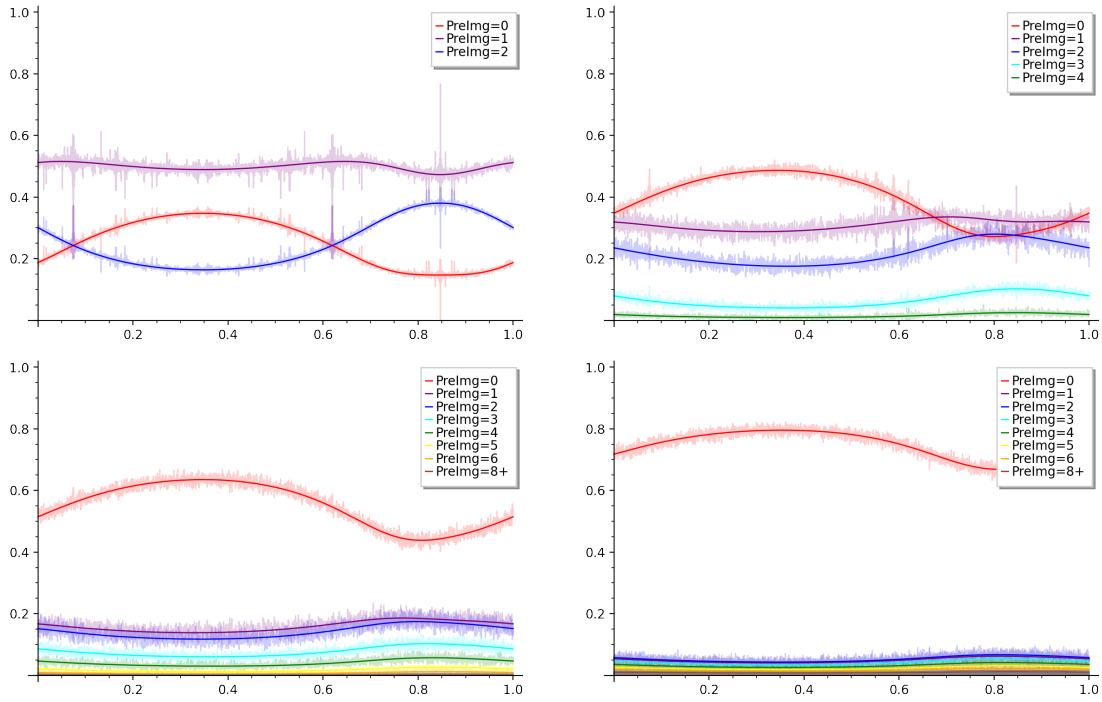

FIGURE 11. These curves represent the local densities of the number of preimages. The expected theoretical values given by Proposition 6 — and computed with the help of Proposition 7 — are represented in full colors. The actual values for the map are in light colours, they represent the quantity (8) for $R = 40$ and $N = 10^6$. The different graphs correspond to different times: from left to right and top to bottom, $k = 1, 2, 4$ and 10.

In this case, the generating series formalism gives the following nice formula, that allows to compute the distributions a_m by an iterating process involving the RPF operator L_f.

Proposition 7. *If $d = 2$, then, denoting $f^{-1}(y) = \{x_0, x_1\}$,*

$$\begin{aligned}\overline{P}_{k+1}(y) =& \frac{1}{f'(x_0)}\left(1 - \frac{1}{f'(x_1)}\right)\overline{P}_k(x_0) + \frac{1}{f'(x_1)}\left(1 - \frac{1}{f'(x_0)}\right)\overline{P}_k(x_1)\\ &+ \frac{1}{f'(x_0)f'(x_1)}\overline{P}_k(x_0)\overline{P}_k(x_1)\\ &+ \left(1 - \frac{1}{f'(x_0)}\right)\left(1 - \frac{1}{f'(x_1)}\right)\end{aligned}$$

Hence, denoting $\overline{Q}_k = \overline{P}_k - 1$,

$$\overline{Q}_{k+1} = \frac{1}{2}\left(L_f(\overline{Q}_k)\right)^2 + L_f\left(\overline{Q}_k - \frac{1}{2}\frac{\overline{Q}_k^2}{f'}\right).$$

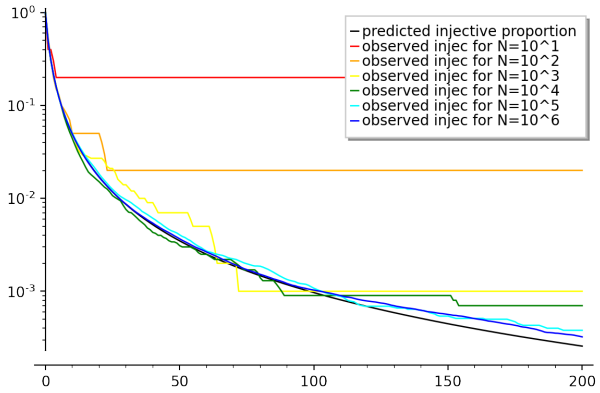

FIGURE 12. Proportion of points of E_N with one preimage under f_N^k (the coloured curves) depending on k, for 6 different values of N: $10^1, 10^2, 10^3, 10^4, 10^5$ and 10^6. We also represent the theoretical value (given by Proposition 6, black curve) depending on k in logaritmic scale.

Proof. Direct computation of the probabilities. □

This proposition gives a fast algorithm to compute the distributions a_m, as it allows to get it from iterations of L_f for which we have a fast algorithm.

Figure 11 gathers both theoretical and real values of the local densities of preimages. For the actual values, we represent the quantities, for different integers m, for a fixed discretization size N and a fixed time k,

$$\frac{1}{2R}\,\mathrm{Card}\left\{y \in E_N \cap [x - R/N, x + R/N] \;\middle|\; \mathrm{Card}\, f_N^{-k}(y) = m\right\}. \tag{8}$$

As can be seen on this figure, the predictions of Proposition 6 are quite accurate: the theoretical and actual curves match very well, up to time 10, for $N = 10^6$. In fact, these predictions stay accurate during quite a long time, as can be observed on Figure 12: for $N = 10^5$ or $N = 10^6$, there is no big difference between the observed values and the prediction up to time 200. In fact, it seems that the theoretical predictions of Figures 10 and 12 stay accurate until a time comparable to $\sqrt{N}$.

Moral. The predictions of Theorem 3 and Propositions 4 and 6 stay accurate until a time proportional to $\sqrt{N}$.

This suggests that the discretizations begin to deviate from these theoretical predictions when there is a significant proportion of points of E_N that have fallen in a periodic orbit of f_N.

4. Medium term behaviour

In [Lan98], Oscar E. Lanford proposes to study the dynamics of the maps f_N^t in the regime $\log N \ll t \ll N$. Note that in the view of the discussion of Section 5, one might be tempted to replace the last condition by $\log t \ll \log N$, as sugested by Lanford himself (see also Figure 16 and the associated discussion). For the first condition $\log N \ll t$, it is also justified by the previous study of the short term behaviour, as well as [Gui15a, Theorem 12.17].

For now, theoretical breakthroughs in Landford's regime seem out of reach, which motivates a numerical study of discretizations in this case.

Recall the different phenomena isolated in the introduction, that can explain why the action of discretizations f_N on measures differ from the one of the initial map f.

- (P_1) The iterates of points always belong to E_N.
- (P_2) Two points of E_N having the same image by f_N will have identical positive orbits.
- (P_3) The local shape around $y \in \mathbf{S}^1$ of the image $f_N(E_N)$ is very similar to the one of a linearization of f around the points $f^{-1}(y)$, which is a model set (see [GM22]).
- (P_4) Any point eventually falls in a periodic cycle.

4.1. Different discretization schemes.

To understand what influences the evolution of the distance $\mathrm{d_C}$ between iterates of Lebesgue measure and iterates of the uniform measure under discretizations, we look at what happens when we change the definition of the discretized map. We will need the following notation: for $x \in E_N$, the integer i_x is chosen such that $i_x/N \leq f(x) < (i_x+1)/N$; it allows to set $\epsilon_x \in [0,1]$ such that $f(x) = (i_x + \epsilon_x)/N$.

- `MapToClosest`: This is the already defined discretization f_N of the map, where $f_N(x)$ is defined as the point of E_N closest to $f(x)$.
- `OnceDecidedRandom`: $D_N^o(f) : E_N \to E_N$ is a random map, such that for each $x \in E_N$, the point $D_N^o(f)(x)$ is chosen *once for all* and randomly (and independently) to be i_x/N with probability $1-\epsilon_x$, and to be $(i_x+1)/N$ with probability ϵ_x. Note that the iterations of two points $x, y \in E_N$ under $[D_N^o(f)]^2$ are independent iff $D_N^o(f)(x) \neq D_N^o(f)(y)$.
- `StepwiseRandom`: $D_N^s(f) : E_N \to E_N$ is a random map quite similar to $D_N^o(f)$ (`OnceDecidedRandom`), such that for each $x \in E_N$ *and at each iteration*, the point $D_N^s(f)(x)$ is chosen randomly (and independently) to be i_x/N with probability $1-\epsilon_x$, and to be $(i_x+1)/N$ with probability ϵ_x.
- `PointsRandomOnGrid`: $D_N^g(f)$ acts independently on N-tuples of elements of E_N as $D_N^s(f)$ (`StepwiseRandom`):

$$D_N^g(f)(x_1, \dots, x_N) = \big(D_N^s(f)(x_1), \dots, D_N^s(f)(x_N)\big).$$

  Of course, this gives the measure

$$\frac{1}{N}\sum_{i=0}^{N-1} \delta_{[D_N^s(f)]^k(i/N)}.$$

- `PointsPerturbed`: $D_N^p(f)$ acts on N-tuples of elements of $\mathbf{S}^1$ as a random perturbation of f: let $\tilde{f}_N$ be the random map obtained from f by post-composing

with a uniform noise on the segment $[-1/(2N), 1/(2N)]$ (*i.e.* $\tilde{f}_N(x)$ is chosen randomly and uniformly in $[f(x) - 1/(2N), f(x) + 1/(2N)]$). Then

$$D^p_N(f)(x_1, \dots, x_N) = \big(\tilde{f}_N(x_1), \dots, \tilde{f}_N(x_N)\big).$$

- `MapToCombination`: $D^c_N(f)$ acts only on the measures on E_N. It is affine, in the sense that for any convex combination $\mu = \sum_i \lambda_i \delta_{x_i}$, one has $D^c_N(f)(\mu) = \sum_i \lambda_i D^c_N(f)(\delta_{x_i})$. And $D^c_N(f)(\delta_x)$ is defined by

$$D^c_N(f)(\delta_x) = (1 - \epsilon_x)\delta_{i_x/N} + \epsilon_x \delta_{(i_x+1)/N}.$$

Let us discuss the fundamental differences between these maps.

`MapToClosest` and `OnceDecidedRandom` have a quite similar definition, except that the first one is deterministic and the second one random. More precisely, there is the following difference between these maps: as f is almost linear at a small scale, the image of $(i+1)/N$ under f_N will depend *deterministically* on $f(i/N) \mod N$, while the image of $(i+1)/N$ under $D^o_N(f)$ will depend only *probabilistically* on $f(i/N) \mod N$. In other words, for N large enough, $f_N(E_N)$ is locally almost (*i.e.* up to a set of arbitrarily small local density) a *model set* (for a definition and a study of this property, see [GM22] or [Gui19]), a property that $D^o_N(f)(E_N)$ does not possess. This will allow us to determine if the phenomenon (P_3) has a detectable effect on the evolution of the distance $\mathrm{d_C}$ (1) between $(f^k_N)_*(\mathrm{Leb}_N)$ and $f^k_*(\mathrm{Leb})$.

The difference between `OnceDecidedRandom` and `StepwiseRandom` is that the second one is not autonomous. Hence, almost surely, orbits for this map will not be pre-periodic, while all orbits of `MapToClosest` and `OnceDecidedRandom` are. This will allow us to determine if the phenomenon (P_4) has an effect on the evolution of the distance (1).

An important feature of the three previous maps (`MapToClosest`, `OnceDecidedRandom` and `StepwiseRandom`) is that orbits that merge then stay together forever. The map `PointsRandomOnGrid`, which besides is quite similar to `StepwiseRandom`, does not have this property. A priori, $D^g_N(f)(x) = D^g_N(f)(y)$ does not imply that $[D^g_N(f)]^2(x) = [D^g_N(f)]^2(y)$ a.s. This will allow us to determine if (P_2) affects the evolution of the distance (1).

All the four previous maps are based on the discretization grid E_N. This is not the case for `PointsPerturbed`, which acts on N-tuples of points of the circle. It can be seen as a continuous counterpart of `PointsRandomOnGrid`. This will allow us to determine if the phenomenon (P_1) affects the evolution of (1).

Finally, `MapToCombination` is the only discretization type which splits measures [3].

Figure 13 shows the evolution of the distance $\mathrm{d_C}$ between the measures $f^k_*(\mathrm{Leb})$ and the images of Leb_N under the iterates of the different discretization types of f: f_N, $D^o_N(f)$, $D^s_N(f)$, $D^g_N(f)$, $D^p_N(f)$ and $D^c_N(f)$.

On the left of this figure, where $N = 750$, there is no intermediate regime for the discretizations f_N and $D^o_N(f)$: from time $k \simeq 100$, the distance evolution becomes periodic. This can be explained by the fact that from this time, most of the grid's points have fallen in a few cycles of the discretization: one directly jumps from the small term behaviour, which is described quite well by Theorem 2, to the periodic asymptotic regime. Indeed, in this case the limit time of short-term behaviour should be around

[3] By Perron-Frobenius theorem, the measures obtained from `MapToCombination` tend (when the time goes to infinity) to some measure depending on N. We do not know if these measures tend to SRB when N goes to infinity. It may be possible to prove it using the ideas of [GN14], by checking that the distance between both Perron-Frobenius and discretized (associated to `MapToCombination`) transfer operators are close relative to BV_1 distance. As this is not in the scope of this article, we do not investigate this question.

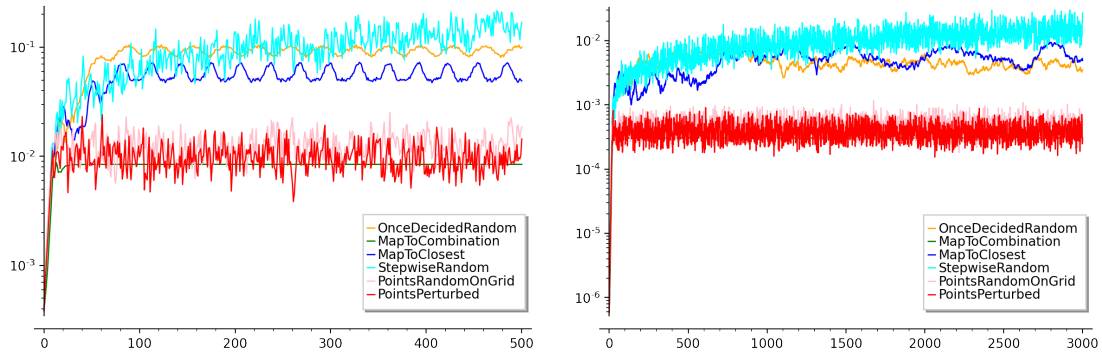

FIGURE 13. Distance $\mathrm{d_C}$ between the measures $f_*^k(\mathrm{Leb})$ and the images of Leb_N under f_N^k and $(D_N^i(f))^k$ for $i \in \{o, s, g, p, c\}$ depending on the time k. On the left graphic, $N = 750$ and on the right one, $N = 50\,000$.

$\log_2 N \simeq 10$, while the theoretical average time for orbits to cycle is $\sqrt{\pi N/2} \simeq 34$ (see Section 5).

For $N = 50\,000$ (Figure 13, right), this periodic asymptotic behaviour does not appear clearly for time $k \leq 3\,000$: there is an actual medium term behaviour of discretizations.

Before studying further this intermediate regime, we first examine random point processes in the point of view of the distance $\mathrm{d_C}$ with the initial measure.

4.2. **Cramér distance between a measure and the random point process associated to it.** We have seen that on the simulations we made, the theoretical estimates on the local distributions of preimages (Paragraphs 3.2 and 3.3) stay relevant in the middle term. Hence, they can be used to set a conjectural behaviour of the distance $\mathrm{d_C}$ in the middle term. Let us first introduce some definitions.

Let $\tilde{\mu}_1, \dots, \tilde{\mu}_M$ be probability measures on $\mathbf{S}^1$, with the density of $\tilde{\mu}_m$ being given by the map $a_m / \int_{Sp^1} a_m$ (recall that a_m was defined in (7) and described in Proposition 6). Let $K \in \mathbf{N}$, $(m_i)_{1 \leq i \leq K} \in \{1, \dots, M\}^K$, and set $N = \sum_{i=1}^K m_i$. Let also ν_μ be the random probability measure defined by

$$\nu_\mu = \frac{1}{N} \sum_{i=1}^{K} m_i \delta_{p_i},$$

where each point p_i is chosen independently in $\mathbf{S}^1$, according to the measure $\tilde{\mu}_{m_i}$. Suppose that for any m,

$$\mathrm{Card}\{i \mid m_i = m\} \simeq \int_{\mathbf{S}^1} a_m$$

(meaning that we have this asymptotics when N goes to infinity).

Conjecture 8. *In the regime* $\log N \ll t$ *and* $\log t \ll \log N$*, the distance*(1) *is close to the expected value of the Cramér distance between the SRB measure and* ν_μ*.*

As a first step, before getting to the numerical study, we compute the expected value of the square of distance $\mathrm{d_C}$ between the SRB measure and ν_μ.

Let μ be a probability measure on $\mathbf{S}^1$. We identify $\mathbf{S}^1$ with $[0, 1]$, and define f as[4] the cumulative distribution function of μ minus its average (so that $\int_0^1 f = 0$). Let also F

[4]There is a conflict of notations with the dynamics f, we hope that which one is used is clear from the context.

be the antiderivative of f such that:

$$F(x) = \int_0^x f(t)\,\mathrm{d}t.$$

Remark that $F(0) = F(1) = 0$, and that $F \leq 0$. Finally, given $p \in \mathbf{S}^1$, one defines $g_p(x) = \chi_{[p,1]}(x) - (1-p)$ to be the cumulative-minus-average distribution function of δ_p

The following theorem gives the expectation of the (square of the) distance $\mathrm{d_C}$ between a measure μ and a point process associated to it.

Theorem 9. *Let μ and $\tilde{\mu}_1, \dots, \tilde{\mu}_M$ be probability measures on $\mathbf{S}^1$ with respective cumulative distribution functions f and $\tilde{f}_1, \dots, \tilde{f}_M$.*

Let $(m_i)_{1\leq i\leq K} \in \{1, \dots, M\}^K$, and set $N = \sum_{i=1}^K m_i$. Let also ν_μ be the random probability measure defined by

$$\nu_\mu = \frac{1}{N}\sum_{i=1}^K m_i \delta_{p_i},$$

where the points p_i are chosen independently in $\mathbf{S}^1$, each one with distribution $\tilde{\mu}_{m_i}$. Then

$$\begin{aligned}\mathbf{E}\left[\mathrm{d_C}(\mu,\nu_\mu)^2\right] &= \int_0^1 \left(f - \sum_{i=1}^K \frac{m_i}{N}\tilde{f}_{m_i}\right)^2 - \sum_{i=1}^K \frac{m_i^2}{N^2}\int_0^1 \left(\tilde{f}_{m_i}^2 + 2\tilde{F}_{m_i}\right)\\ &= \mathrm{d_C}\left(f, \sum_{i=1}^K \frac{m_i}{N}\tilde{f}_{m_i}\right)^2 + \sum_{i=1}^K \frac{m_i^2}{N^2}\left(\frac{1}{12} - \mathrm{d_C}\left(\tilde{f}_{m_i}, \mathrm{Leb}\right)^2\right). \qquad (9)\end{aligned}$$

The proof of this theorem can be found in appendix.

The setting of this theorem will be applied in the case where μ can be written as $\mu = \sum_{m=0}^M m_i\mu_i$ (hence the μ_i are not probability measures), and the measures $\tilde{\mu}_i$ are the normalizations of the μ_i, with the m_i being chosen such that the normalization factors are close to m_i/N (see Remark 10).

Some similar estimations were obtained for the Wasserstein distance W_1 in [BL19], but the authors only manage to get bounds ant not exact values for the expected value.

Remark 10. Note that N being fixed, one can choose the family m_i such that the first term is of order C/N^2, while the second one is typically of order $1/N$.

Indeed, suppose that the cumulative distribution function f of μ satisfies $f = \sum_{m=1}^K \lambda_m \tilde{f}_m$, and for $p \in \mathbf{N}$, let (m_i) such that

$$\mathrm{Card}\{i \mid m_i = m\} = \lfloor p\lambda_m \rfloor.$$

Note that

$$\frac{p\lambda_m - 1}{\sum_{n=1}^K (p\lambda_n + 1)} \leq \frac{\lfloor p\lambda_m\rfloor}{\sum_{n=1}^K \lfloor p\lambda_n\rfloor} \leq \frac{p\lambda_m + 1}{\sum_{n=1}^K (p\lambda_n - 1)},$$

so

$$-\frac{1+K}{p+K} \leq \frac{\lfloor p\lambda_m\rfloor}{\sum_{n=1}^K \lfloor p\lambda_n\rfloor} - \lambda_m \leq \frac{1+K}{p-K},$$

and

$$\left\| f - \sum_{m=1}^K \frac{\lfloor p\lambda_m\rfloor}{\sum_{n=1}^K \lfloor p\lambda_n\rfloor}\tilde{f}_m \right\|_2 \leq \sum_{m=1}^K \left|\frac{\lfloor p\lambda_m\rfloor}{\sum_{n=1}^K \lfloor p\lambda_n\rfloor} - \lambda_m\right| \|\tilde{f}_m\|_2 \leq K\frac{1+K}{p-K}.$$

Hence,

$$\left\| f - \sum_{m=1}^K \frac{\lfloor p\lambda_m\rfloor}{\sum_{n=1}^K \lfloor p\lambda_n\rfloor}\tilde{f}_m \right\|_2^2 = O\left(\frac{1}{p^2}\right),$$

which gives a distance of the order of $1/p^2$ by Lemma 1.

On the other hand,

$$\sum_{m_i=m} \frac{m_i^2}{N^2} = m^2 \frac{\lfloor p\lambda_m \rfloor}{\sum_{n=1}^K \lfloor p\lambda_n \rfloor} \frac{1}{\sum_{n=1}^K \lfloor p\lambda_n \rfloor} \geq \frac{m^2\lambda_m}{p+K}$$

for any p large enough. Hence, in this case, the dominating term in (9) is the second one.

The equality between the two lines of the theorem's equation (9) comes from the following elementary lemma.

Lemma 11. *Let μ be a probability measure on $\mathbf{S}^1$, with distribution function minus average f. Let F be an antiderivative of f such that $F(0) = F(1) = 0$. Then*

$$\int_0^1 (f^2 + 2F) = \mathrm{d_C}\left(\mu, \mathrm{Leb}\right)^2 - \frac{1}{12} \leq 0.$$

A proof of this lemma can be found in appendix.

By taking $m_i = 1$ for any i, one gets the following corollary about point precesses with points of uniform weights.

Corollary 12. *Let μ be a probability measure on $\mathbf{S}^1$, $N \in \mathbf{N}$, and ν_μ be the random measure defined by*

$$\nu_\mu = \frac{1}{N} \sum_{k=1}^N \delta_{p_k},$$

where the p_k's are iid points with distribution μ. Then

$$\mathbf{E}\left[\mathrm{d_C}(\mu, \nu_\mu)^2\right] = \frac{1}{N}\left(\frac{1}{12} - \mathrm{d_C}\left(\mu, \mathrm{Leb}\right)^2\right). \tag{10}$$

Remark 13. A simple computation shows that the square of the distance $\mathrm{d_C}$ between N equispaced points and Lebesgue measure, is equal to $1/(12N^2)$. On the other hand, one has $\mathbf{E}\left[\mathrm{d_C}(\mathrm{Leb}, \nu_{\mathrm{Leb}})^2\right] = 1/(12N)$.

Hence, the expectation of the square of the Cramér distance of the uniform point process (with all weights equal to 1) is $1/(12N)$. In this case, the squared distance ${\mathrm{d_C}}^2$ for a typical point process is way bigger than the minimal squared distance ${\mathrm{d_C}}^2$ for the same number of points (it is of the order of its square).

4.3. **Comparison between the random point process and the discretization.** Now we have defined different discretization types in Paragraph 4.1 and got a theoretical estimate of the distance $\mathrm{d_C}$ between a measure and the random point process associated to it paragraph 4.2, we can compare them numerically.

Figure 14 displays the mean values as well as the mean values $\pm$ standard deviation of the Cramér distance between the iterates of the discrete measure by the discretization type and the iterate of Lebesgue measure by RPF operator, for all the discretization types defined in Paragraph 4.1.

It also shows the the theoretical prediction for small times given by Theorem 2, and the curves of two expected values of the distance $\mathrm{d_C}$ between SRB measure and a point process. The first one, in violet, is obtained from Corollary 12 ; it is square root of the expected value of the square of the distance between the SRB measure and the measure made of N independent random points with respect to this SRB measure. The second one, in pink, is cooked from Theorem 9 and the local distribution of preimages given by Proposition 6 in the following way: for each time k, we compute the theoretical local distribution of preimages $a_i = a_i(y,k)$ by the algorithm given by Proposition 7.

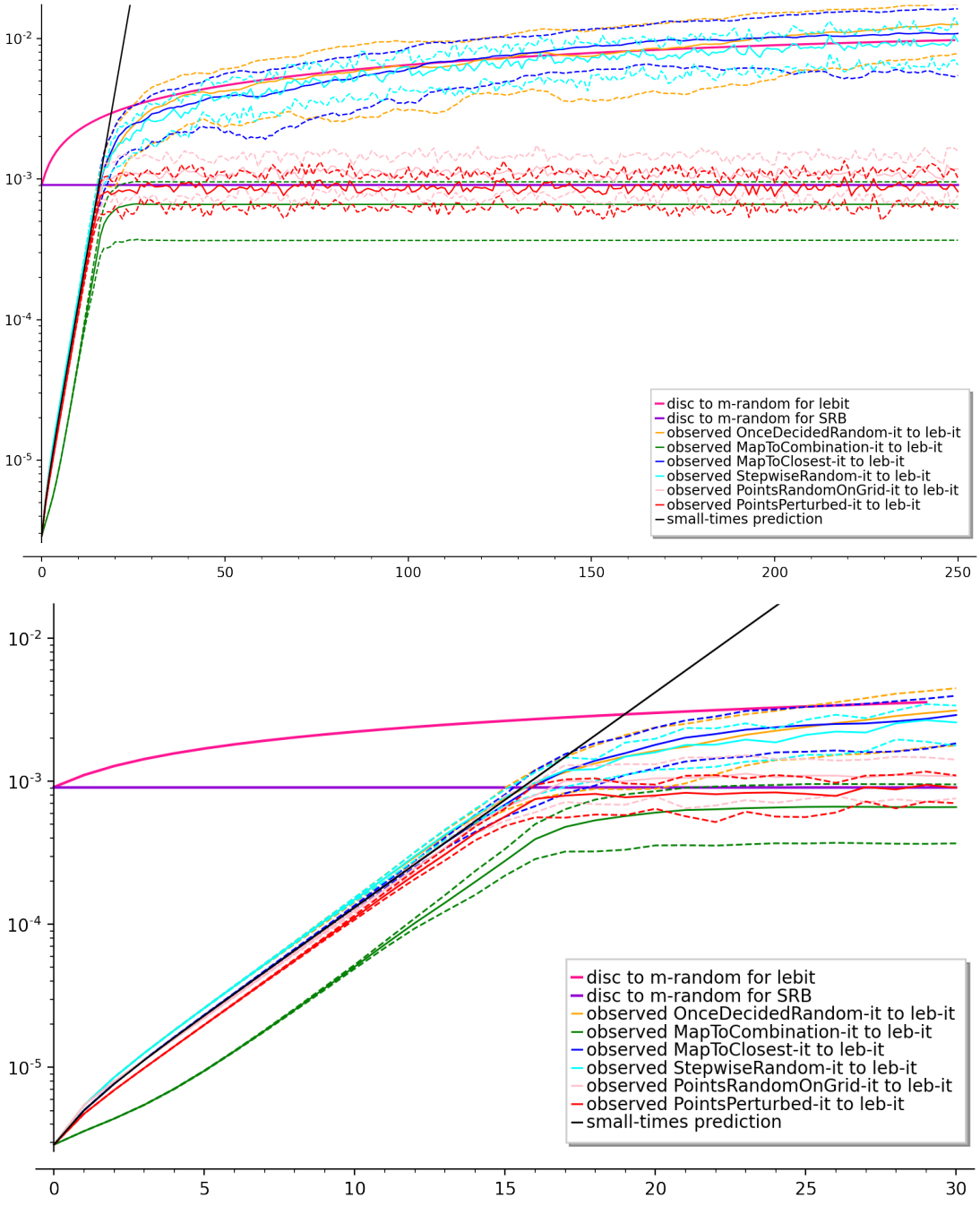

FIGURE 14. The bottom graphic is a zoom of the top one for small times. In these simulations, $N = 10^5$. Each trio of curves of the same color (one in plain line and two dashed) is similar to the curves of Figure 7: it represents the mean (plain) and the mean $\pm$ standard deviation (dashed) of the distance $\mathrm{d_C}$ between the iterates of the discrete measure by the discretization type and the iterate of Lebesgue measure by RPF operator. The black curve is, as the red curve of Figure 7, the theoretical prediction given by Theorem 2. The violet curve "disc to m-random for SRB" is the expected value of the distance between the SRB measure and N random points with respect to this SRB measure, it is given by Corollary 12. The pink curve "disc to m-random for lebit" is obtained from Theorem 9 (see the map $p(k)$ defined in Equation (11)).

To each of these functions $a_i(y,k)$, which represent local densities of measures (which we normalize to get probability measures), are associated a cumulative distribution functions $\tilde{f}_i^k$. This allows to get an estimation by means of (9) (see also Remark 10)

$$p(k) = \sum_{i=1}^{K} \left(\int_{\mathbf{S}^1} a_i(y,k)\,\mathrm{d}y \right)^2 \left(\frac{1}{12} - \mathrm{d_C}\left(\tilde{f}_i^k, \mathrm{Leb} \right)^2 \right). \tag{11}$$

At first glance, we can group the discretization types in three different clusters.

(C1) A first one containing only `MapToCombination`, whose asymptotic behaviour looks stationary, the asymptotic average distance is smaller than the estimation `disc to m-random for SRB`.

(C2) A second one containing `PointsRandomOnGrid` and `PointsPerturbed`. These two types of discretization give asymptotic behaviours similar to the estimation `disc to m-random for SRB`.

(C3) A third one containing `MapToClosest`, `OnceDecidedRandom` and `StepwiseRandom`. These three types of discretization behave asymptotically more or less as `disc to m-random for lebit` given by the map $p(k)$.

However, a closer look at each cluster reveals small differences.

For (C2), while the average value for `PointsPerturbed` follows asymptotically very well the curve of `disc to m-random for SRB`, the discretization type `PointsRandomOnGrid` has a significantly greater average asymptotic value. This is quite unexpected, as the difference induced by replacing the SRB measure by the projection of it on E_N (by mean of E_N) in Corollary 12 is of order $1/N^2$, and hence is negligible with respect to the orders of the computed distances, which are of order $1/N$. We have no explanation to this phenomenon.

For (C3), the curves associated to `MapToClosest` and `OnceDecidedRandom` are very similar (see also Figure 15). Hence, the already discussed difference between microscopic behaviours of these discretizations, the first one having deterministic local correlations and the second one random local correlations, seems to have no impact on the asymptotics of the distance $\mathrm{d_C}$ between measures. Moreover, the curves corresponding to `StepwiseRandom`, although also following quite well the curve of $p(k)$, behaves a bit more erratically than the two other ones (this is even more blatent on Figure 13).

Simulations over a larger time range show that the average distance for `StepwiseRandom`, form a certain point, gets bigger than the one for `MapToClosest` and `OnceDecidedRandom`. More precisely, Figure 15 shows this distance for times $t \leq 2000$ and $N = 120\,000$. On this simulation, we can see that this time where the mean distances start to be different is more or less 1000. This time is to be compared with the mean time necessary for an orbit to cycle for a typical map of 120 000 elements, which is $\sqrt{\pi N/2} \simeq 137$: from this time 137, a significant part of orbits have cycled, which perturbs the process of injectivity loss. Note that on Figure 15 we have not represented the prediction that we discussed in the beginning of this paragraph, as in this time range accurate computations are out of our machine capacities: in the simulations we have to truncate the series a_i up to some $i \leq i_0$ to avoid exponential explosion of data depending on simulation time; we checked empirically that this truncation does not affect the prediction by verifying that the predictions are the same weather we truncate up to i_0 or $2i_0$. The threshold we chose for the simulations ($i_0 = 256$) gives similar results to $2i_0 = 512$ for times ≤ 250 (as in Figure 14) but not $\leq 2\,000$ (as in Figure 15); a larger threshold for time 2 000 would make the computations extremely long and memory costing.

From these observations, one can conclude the following moral.

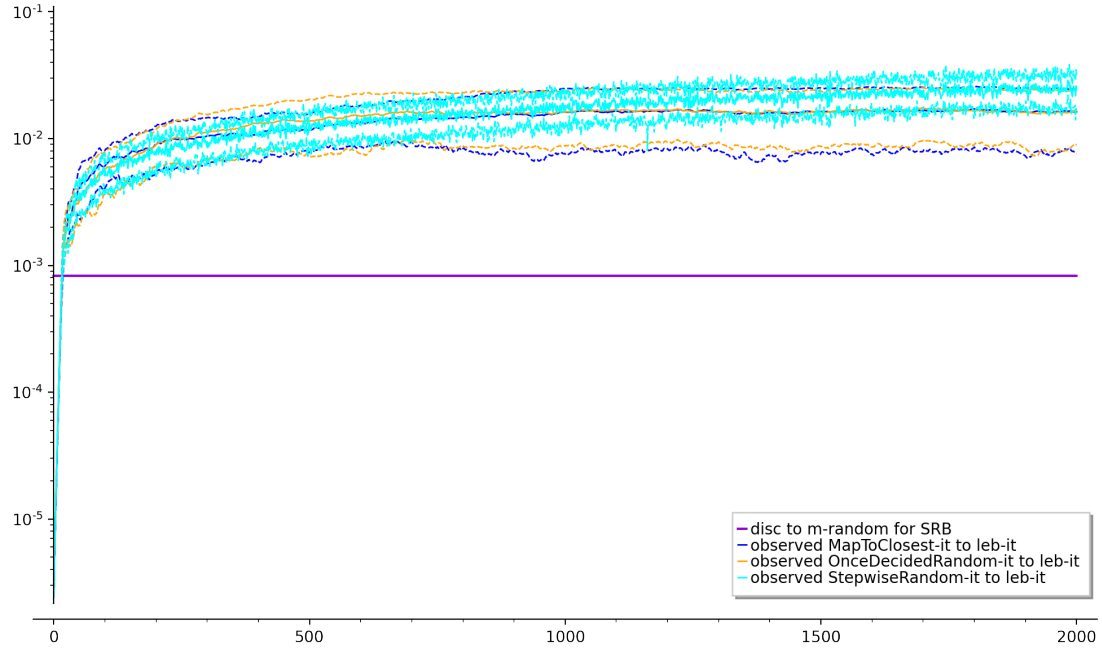

FIGURE 15. This figure shows the same curves as Figure 14 for $N = 120\,000$ but only for `MapToClosest`, `OnceDecidedRandom` and `StepwiseRandom`.

Moral. The main phenomenon influencing the middle term behaviour of $(f_N^k)^*(\mathrm{Leb}_N)$ is the fact that orbits under f_N merge. More precisely, the distance $\mathrm{d_C}$ between $(f^k)^*(\mathrm{Leb})$ and $(f_N^k)^*(\mathrm{Leb}_N)$ is rather well described by the distance $\mathrm{d_C}$ between the SRB measure and the point process described by $p(k)$ (see (11)): locally around $y \in \mathbf{S}^1$, the proportion of points with weight i of this process is equal to $a_i(y,k)$, where $a_i(y,k)$ represents the local proportion of points around y that have i preimages under f_N^k.

Note that in the simulations we performed the "middle term" is not that long and it may be that the phenomena specific to the short and long term still interfere in the time range and the discretization orders we chose: as noticed in Figure 13, left, for smaller orders N there is even no middle term transitory behaviour. We would need more computing power to test the validity of the prediction (11) on bigger orders N (typically close to 10^7).

5. Long term behaviour

From Figure 3, one can wonder whether the quantity

$$\limsup_{k\to+\infty} \mathrm{d_C}\left((f_N)_*^k(\mathrm{Leb}_N), \mathrm{SRB}\right),$$

which depends on N, tends to 0 when the discretization parameter N goes to infinity or not. According to the simulations (see Figure 17), it seems that yes, but unfortunately the proof of this result seems unreachable for now.

Let us first recall the fact that the maps f_N are finite, so that every orbit eventually falls in a periodic cycle. Hence, one can characterize the expression "asymptotic regime" by the fact that all points have already browsed a whole periodic orbit[5]. Figure 16 shows the average of this time over points of E_{2^k} depending on k.

[5]In practical, we will see the asymptotic regime's behaviour as soon as *most of* points of E_N already have browsed a whole cycle.

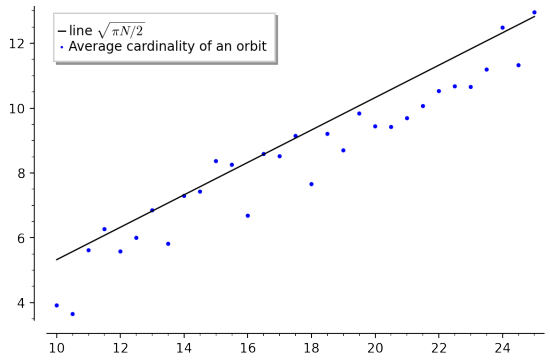

FIGURE 16. $\log_2$ of the average time needed for an orbit of f_{2^k} to cycle (*i.e.* average cardinality of an orbit) depending on k (blue points). This behaves quite the same as the same quantity for a typical random map on a set of 2^k elements (black line).

One can observe that this quantity behaves more or less as the same quantity for a typical random map on a set of N elements, which is equivalent to $\sqrt{\pi N/2}$ (see [Bol01]); this equivalent is represented in black in Figure 16. This quantity is around 10^8 for $N = 2^{56}$ (which is the classical precision used by computers). Hence, in practical, one usually does not reach the asymptotic regime when iterating a map.

There is a canonical measure associated to the asymptotic regime in the following way. Fix $N > 0$, and let Leb_N be the uniform measure on the grid E_N. The measures $(f_N)^n_*(\mathrm{Leb}_N)$ converge in the Cesàro mean towards a measure

$$\mu_N = \lim_{k\to+\infty} \frac{1}{k} \sum_{n=0}^{k-1} (f_N)^n_*(\mathrm{Leb}_N). \tag{12}$$

This measure is supported in the union of the periodic cycles of f_N, the total weight of each of them being proportional to the size of its basin of attraction.

Question 14. *Do we have $\mu_N \to_{N\to+\infty}$ SRB (in the weak-* topology) for a generic C^r expanding map f?*

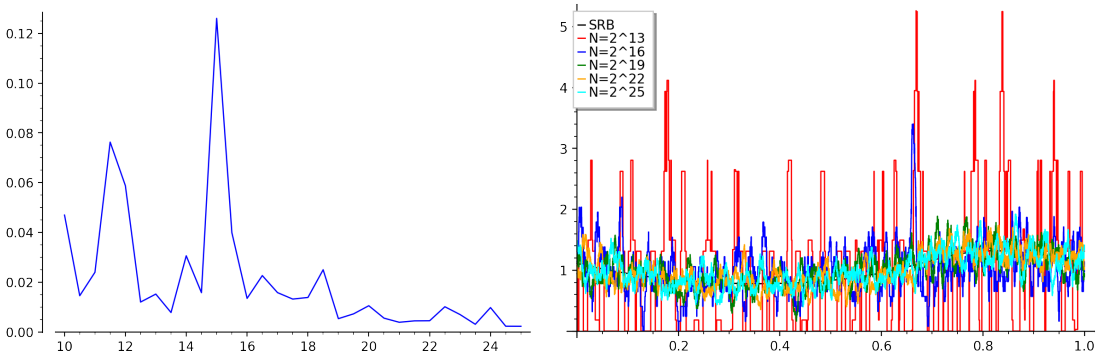

FIGURE 17. Left: Cramér distance between the measures SRB and μ_{2^k} depending on k. We do not have any explanation for the threshold $k = 15$. Right: densities of the measures μ_{2^k}, for $k = 13, 16, 19, 22, 25$, versus density of the SRB measure.

Numerical experiments suggest that the answer to this question might be yes, as shown by Figure 17. Note that the convergence, if happens, is extremely slow: it would give a terrible algorithm to compute an approximation of the SRB measure.

However, it is possible that these simulations are misleading. As observed in [Gui15a] (see Figures 12.14 and 12.17), for some C^1 area-preserving diffeomorphisms of the torus, the measures μ_N seem to converge to the area for a set of N of density 1, but there are still rare values of N for which the distance between μ_N and the area stay at positive distance. Such a behaviour can be observed on Figure 18: while for most of the 100 discretization orders N between 2^{20} and $2^{20}+99$, the distance between the SRB measure and μ_N is around 0.01, for two of these discretization orders, the distance is bigger than 0.05 (a distance that is no longer attained after 2^{15} on Figure 17).

Moral. Our simulations do not suggest a clear conjecture about the convergence or not of μ_N towards SRB, but it seems that this convergence holds for a subsequence of N of density 1.

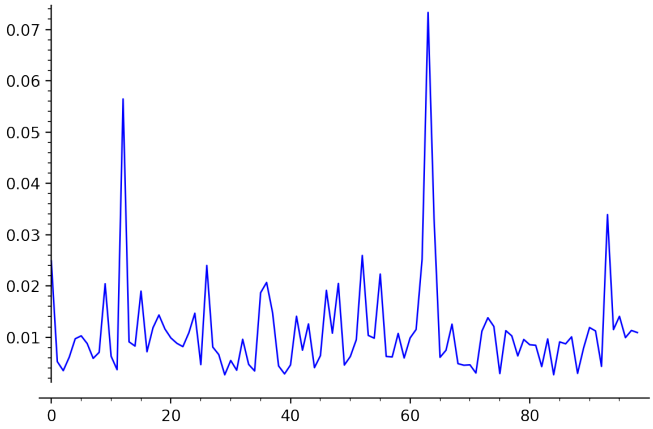

FIGURE 18. Cramér distance between the measures SRB and $\mu_{2^{20}+i}$, depending on $0 \leq i \leq 99$.

APPENDIX A. PROOF OF THEOREM 9 AND LEMMA 11

We start with the proof of Lemma 11, some facts of it being used in the one of Theorem 9.

Proof of Lemma 11. One has

$$\begin{aligned}
\mathrm{d_C}\left(\mu, \mathrm{Leb}\right)^2 &= \int_0^1 \left(f(x) + \frac{1}{2} - x\right)^2 \mathrm{d}x \\
&= \int_0^1 f^2 + 2\int_0^1 \left(\frac{1}{2} - x\right) f(x)\,\mathrm{d}x + \int_0^1 \left(\frac{1}{2} - x\right)^2 \mathrm{d}x \\
&= \int_0^1 f^2 - 2\int_0^1 x f(x) + \frac{1}{12} \\
&= \int_0^1 (f^2 + 2F) + \frac{1}{12} \qquad \text{(by parts)},
\end{aligned}$$

so

$$\int_0^1 (f^2 + 2F) = \mathrm{d_C}\left(\mu, \mathrm{Leb}\right)^2 - \frac{1}{12}.$$

This proves the equality of the lemma.

We now prove the inequality. We first suppose that f is a convex combination of maps g_p, where $g_p(x) = \chi_{[p,1]}(x) - (1-p)$ is the cumulative-minus-average distribution function of δ_p. For g_p we have the equality

$$\langle g_p, g_p \rangle = p(1-p) = -2\int G_p.$$

If $f = \sum_i \lambda_i g_{p_i}$, with $p_i \in \mathbf{S}^1$ and $\lambda_i \geq 0$, $\sum_i \lambda_i = 1$, then

$$\begin{aligned}\int (f^2 + 2F) &= \langle \sum_i \lambda_i g_{p_i}, \sum_j \lambda_j g_{p_j} \rangle + 2 \sum_i \lambda_i \int G_{p_i} \\ &= \sum_{i,j} \lambda_i \lambda_j \langle g_{p_i}, g_{p_j} \rangle - \sum_i \lambda_i \langle g_{p_i}, g_{p_i} \rangle \\ &= \sum_{i,j} \lambda_i \lambda_j \langle g_{p_i}, g_{p_j} - g_{p_i} \rangle.\end{aligned}$$

Notice that fixing $p \leq q$, we have

$$\begin{aligned}\langle g_p, g_q \rangle &= \int_0^p (p-1)(q-1)\,\mathrm{d}x + \int_p^q p(q-1) + \int_q^1 pq \\ &= p(p-1)(q-1) + (q-p)p(q-1) + (1-q)pq \\ &= p(1-q), \qquad (13)\end{aligned}$$

so for any p, q we have $\langle g_p, g_q \rangle \geq \langle g_p, g_p \rangle$. This proves that $\int (f^2 + 2F) \leq 0$ in the case f is a convex combination of maps g_p. The general case comes from the density (in L^2 norm) of such convex combinations among zero-average maps.

Note that a simple additional argument shows that we have equality $\int (f^2 + 2F) = 0$ iff $f = g_p$ for some $p \in \mathbf{S}^1$. □

Proof of Theorem 9. Given two probability measures μ and ν, the square ${\mathrm{d_C}}^2$ of their Cramér distance is obtained as

$$\int_0^1 (f(x) - g(x))^2\,\mathrm{d}x$$

where f, g are the cumulative distribution function minus their average (as defined before Theorem 9). In our case we want to compute the expectation of the square ${\mathrm{d_C}}^2$ of the Cramér distance between the measure μ and the random measure ν_μ (which depends on the random points p_i). In this case, the (random) function g is given by

$$g(x) = \frac{1}{N} \sum_{i=1}^K m_i g_{p_i}(x) = \sum_{i=1}^K \lambda_i g_{p_i}(x),$$

where $g_p(x) = \chi_{[p,1]}(x) - (1-p)$ is the cumulative-minus-average distribution function of δ_p, and $\lambda_i = \frac{m_i}{N}$ (note that they satisfy $\sum_i \lambda_i = 1$). Each point p_i will be chosen randomly and independently with distribution $\tilde{\mu}_{m_i}$

First, suppose that the distribution functions $\tilde{f}_m$ of $\tilde{\mu}_m$ are differentiable; in this case $\tilde{f}'_m$ is equal to the density of $\tilde{\mu}_m$. Note that in this case $\tilde{f}'_m \in L^1(\mathbf{S}^1)$, so that all further applications of Fubini's theorem will be valid.

Keeping implicit that we will be averaging over $p_1, \ldots, p_n$ chosen at random in $[0,1]^n$ with distribution $\tilde{f}'_{m_1}(p_1)\,\mathrm{d}p_1 \cdots \tilde{f}'_{m_n}(p_n)\,\mathrm{d}p_n$, the square D of the Cramér distance ${\mathrm{d_C}}^2$ can be computed as

$$\begin{aligned}D &= \int_0^1 \left(f(x) - \sum_{i=1}^K \lambda_i g_{p_i}(x) \right)^2 \mathrm{d}x \\ &= \int_0^1 f(x)^2\,\mathrm{d}x - 2 \int_0^1 \sum_{i=1}^K f(x) \lambda_i g_{p_i}(x)\,\mathrm{d}x \\ &\quad + \int_0^1 \sum_{i=1}^K \lambda_i^2 g_{p_i}(x)^2\,\mathrm{d}x + \int_0^1 \sum_{\substack{i,j=1 \\ i \neq j}}^K \lambda_i g_{p_i}(x) \lambda_j g_{p_j}(x)\,\mathrm{d}x \\ &= \int_0^1 f(x)^2\,\mathrm{d}x - 2 \sum_{i=1}^K \lambda_i \int_0^1 f(x) g_{p_i}(x)\,\mathrm{d}x\end{aligned}$$

$$+\sum_{i=1}^{K}\lambda_i^2\int_0^1 g_{p_i}(x)^2\,\mathrm{d}x+\sum_{\substack{i,j=1\\ i\neq j}}^{K}\lambda_i\lambda_j\int_0^1 g_{p_i}(x)g_{p_j}(x)\,\mathrm{d}x.$$

In each integral the average will only be over p_i (or p_i, p_j in the last one), as the integrand does not depend on p_k, for $k \neq i, j$. Each p_i follows the distribution $\tilde{f}'_{m_i}(p)\,\mathrm{d}p$. Therefore we can simplify the sums of equal values and see the integrals as integral in just p (or p, q in the last integral). We can write:

$$\begin{aligned}
D=&\int_0^1 f(x)^2\,\mathrm{d}x-2\sum_i\lambda_i\int_{p=0}^1\int_{x=0}^1 f(x)g_p(x)\tilde{f}'_{m_i}(p)\,\mathrm{d}x\,\mathrm{d}p\\
&+\sum_i\lambda_i^2\int_{p=0}^1\int_{x=0}^1 g_p(x)^2\tilde{f}'_{m_i}(p)\,\mathrm{d}x\,\mathrm{d}p\\
&+\sum_{i\neq j}\lambda_i\lambda_j\int_{p=0}^1\int_{q=0}^1\int_{x=0}^1 g_p(x)g_q(x)\tilde{f}'_{m_i}(p)\tilde{f}'_{m_j}(p)\,\mathrm{d}x\,\mathrm{d}p\,\mathrm{d}q\\
=&I_1-2I_2+\sum_i\lambda_i^2 I_3+\sum_{i\neq j}\lambda_i\lambda_j I_4 \qquad (14)
\end{aligned}$$

Before deducing a general formula we well state two trivial lemmas.

Lemma 15. *For all $a \leq b$ we have:*

$$\begin{aligned}
\int_a^b pf'(p)\,\mathrm{d}p&=\big[pf(p)\big]_a^b-\int_a^b f(p)\,\mathrm{d}p\\
&=bf(b)-af(a)-F(b)+F(a).
\end{aligned}$$

In particular, we get $\int_0^b pf'(p)=bf(b)-F(b)$.

Lemma 16.

$$\int_a^b f'(p)F(p)\,\mathrm{d}p=\big[f(p)F(p)\big]_a^b-\int_a^b f(p)^2\,\mathrm{d}p.$$

In particular we get $\int_0^1 f'(p)F(p)=-\int_0^1 f(p)^2$.

The expression (13) is valid on the half of the square $(p, q) \in [0, 1]^2$ where $p \leq q$, therefore we have (applying the above lemmas and the fact that $F(0) = F(1) = 0$)

$$\begin{aligned}
I_4=&\int_{p=0}^1\int_{q=0}^1\int_{x=0}^1 g_p(x)g_q(x)\tilde{f}'_{m_i}(p)\tilde{f}'_{m_j}(q)\,\mathrm{d}x\,\mathrm{d}q\,\mathrm{d}p\\
=&\int_{q=0}^1\int_{p=0}^q p(1-q)\tilde{f}'_{m_i}(p)\tilde{f}'_{m_j}(q)\,\mathrm{d}p\,\mathrm{d}q+\int_{q=0}^1\int_{p=q}^1 q(1-p)\tilde{f}'_{m_i}(p)\tilde{f}'_{m_j}(q)\,\mathrm{d}p\,\mathrm{d}q \quad \text{(by (13))}\\
=&-\int_{q=0}^1\int_{p=0}^1 pq\tilde{f}'_{m_i}(p)\tilde{f}'_{m_j}(q)\,\mathrm{d}p\,\mathrm{d}q\\
&+\int_{q=0}^1\int_{p=0}^q p\tilde{f}'_{m_i}(p)\tilde{f}'_{m_j}(q)\,\mathrm{d}p\,\mathrm{d}q+\int_{p=0}^1\int_{q=0}^p q\tilde{f}'_{m_i}(p)\tilde{f}'_{m_j}(q)\,\mathrm{d}q\,\mathrm{d}p\\
=&-\left(\int_{p=0}^1 p\tilde{f}'_{m_i}(p)\right)\left(\int_{q=0}^1 q\tilde{f}'_{m_j}(q)\right)\\
&+\int_{q=0}^1\left(q\tilde{f}_{m_i}(q)-\tilde{F}_{m_i}(q)\right)\tilde{f}'_{m_j}(q)\,\mathrm{d}q+\int_{p=0}^1\left(p\tilde{f}_{m_j}(p)-\tilde{F}_{m_j}(p)\right)\tilde{f}'_{m_i}(p)\,\mathrm{d}p\\
=&-\tilde{f}_{m_i}(1)\tilde{f}_{m_j}(1)\\
&+\int_{q=0}^1 q\left(\tilde{f}_{m_i}(q)\tilde{f}'_{m_j}(q)+\tilde{f}_{m_j}(q)\tilde{f}'_{m_i}(q)\right)\mathrm{d}q-\int_{q=0}^1\left(\tilde{F}_{m_i}(q)\tilde{f}'_{m_j}(q)+\tilde{F}_{m_j}(q)\tilde{f}'_{m_i}(q)\right)\mathrm{d}q\\
=&-\tilde{f}_{m_i}(1)\tilde{f}_{m_j}(1) \qquad \text{(by parts, for both integrals)}
\end{aligned}$$

$$+\left[q\tilde{f}_{m_i}(q)\tilde{f}_{m_j}(q)\right]_0^1-\int_0^1\tilde{f}_{m_i}\tilde{f}_{m_j}-\left[\tilde{F}_{m_i}\tilde{f}_{m_j}+\tilde{F}_{m_j}\tilde{f}_{m_i}\right]_0^1+\int_0^1\left(\tilde{f}_{m_i}\tilde{f}_{m_j}+\tilde{f}_{m_j}\tilde{f}_{m_i}\right)$$

(15)
$$=\int_0^1\tilde{f}_{m_i}\tilde{f}_{m_j}$$

For I_3 of (14) we have

$$\begin{aligned}
I_3&=\int_{p=0}^1\int_{x=0}^1 g_p(x)^2\tilde{f}'_{m_i}(p)\,\mathrm{d}x\,\mathrm{d}p\\
&=\int_{p=0}^1 p(1-p)\tilde{f}'_{m_i}(p)\,\mathrm{d}p\\
&=\left[p(1-p)\tilde{f}_{m_i}(p)\right]_0^1+\int_0^1 2p\tilde{f}_{m_i}(p)\,\mathrm{d}p-\int_0^1\tilde{f}_{m_i}(p)\,\mathrm{d}p\quad\text{(by parts)}\\
&=\left[2p\tilde{F}_{m_i}(p)\right]_0^1-\int_0^1 2\tilde{F}_{m_i}(p)\,\mathrm{d}p\quad\text{(by parts)}\\
&=-\int_0^1 2\tilde{F}_{m_i},\qquad(16)
\end{aligned}$$

while for the second integral

$$\begin{aligned}
I_2&=\int_{p=0}^1\int_{x=0}^1 f(x)g_p(x)\tilde{f}'_{m_i}(p)\,\mathrm{d}x\,\mathrm{d}p\\
&=\int_{p=0}^1\int_{x=0}^1 f(x)\chi_{[p,1]}(x)\tilde{f}'_{m_i}(p)\,\mathrm{d}x\,\mathrm{d}p-\int_{p=0}^1\int_{x=0}^1 f(x)(1-p)\tilde{f}'_{m_i}(p)\,\mathrm{d}x\,\mathrm{d}p\\
&=\int_{x=0}^1 f(x)\int_{p=0}^x\tilde{f}'_{m_i}(p)\,\mathrm{d}p\,\mathrm{d}x-\int_{p=0}^1\left(\int_0^1 f(x)\,\mathrm{d}x\right)(1-p)\tilde{f}'_{m_i}(p)\,\mathrm{d}p\\
&=\int_{x=0}^1\left(f(x)\tilde{f}_{m_i}(x)-f(x)\tilde{f}_{m_i}(0)\right)\mathrm{d}x-0\quad\text{(because } f\text{ is zero-average)}\\
&=\int_0^1 f\tilde{f}_{m_i}\qquad(17)
\end{aligned}$$

Joining all simplified expressions (17), (16) and (15), we deduce that (14) can be rewritten as

$$\begin{aligned}
D&=\int_0^1 f^2-2\sum_i\frac{m_i}{n}\int_0^1 f\tilde{f}_{m_i}-2\sum_i\left(\frac{m_i}{n}\right)^2\int_0^1\tilde{F}_{m_i}+\sum_{i\neq j}\frac{m_im_j}{n^2}\int_0^1\tilde{f}_{m_i}\tilde{f}_{m_j}\\
&=\int_0^1\left(f-\sum_i\frac{m_i}{n}\tilde{f}_{m_i}\right)^2-\sum_i\frac{m_i^2}{n^2}\int\left(\tilde{f}_{m_i}^2+2\tilde{F}_{m_i}\right),
\end{aligned}$$

which gives the first formula of the theorem. The second one is a consequence of Lemma 11

We now treat the general case for $\tilde{f}_m$. The cadlag map $\tilde{f}_m$ can be approached in uniform topology by a smooth cumulative distribution function of a measure $\overline{\mu}_m$, which is close to $\tilde{\mu}_m$ in weak-* topology. It then suffices to remark that in (10), the left side is continuous in $\tilde{\mu}_m$ for weak-* topology, and right side is continuous in $\tilde{f}_m$ for the uniform topology. □

References

[Bin92] Philippe M. Binder, *Limit cycles in a quadratic discrete iteration*, Phys. D **57** (1992), no. 1-2, 31–38.

[BL19] Sergey Bobkov and Michel Ledoux, *One-dimensional empirical measures, order statistics, and Kantorovich transport distances*, Memoirs of the American Mathematical Society **261** (2019), 0–0.

[Bla98] Michael Blank, *Discreteness and continuity in problems of chaotic dynamics*, The American mathematical monthly **105** (1998), no. 3, 299– (eng).

[Bol01] Béla Bollobás, *Random graphs*, seconde ed., Cambridge University Press, 2001.

[Boy86] Abraham Boyarsky, *Computer orbits*, Comput. Math. Appl. Ser. A **12** (1986), no. 10, 1057–1064.

[CFM90] Robert M. Corless, Gregory W. Frank, and J. Graham Monroe, *Chaos and continued fractions*, Phys. D **46** (1990), no. 2, 241–253. MR 1083721

[Cor92] Robert M. Corless, *Continued fractions and chaos*, Amer. Math. Monthly **99** (1992), no. 3, 203–215. MR 1216205

[DKKP96] Phil Diamond, Anthony Klemm, Peter Kloeden, and Alexei Pokrovskii, *Basin of attraction of cycles of discretizations of dynamical systems with SRB invariant measures*, J. Statist. Phys. **84** (1996), no. 3-4, 713–733. MR 1400185 (97i:58102)

[DKKP97] Phil Diamond, Victor Kozyakin, Peter Kloeden, and Alexei Pokrovskii, *A model for roundoff and collapse in computation of chaotic dynamical systems*, Math. Comput. Simulation **44** (1997), no. 2, 163–185. MR 1481914 (99a:58114)

[DKP94] Phil Diamond, Peter Kloeden, and Alexei V. Pokrovskii, *An invariant measure arising in computer simulation of a chaotic dynamical system*, J. Nonlinear Sci. **4** (1994), no. 1, 59–68. MR 1258483 (94m:58136)

[DKPV95] Phil Diamond, Peter Kloeden, Alexei V. Pokrovskii, and Alexander Vladimirov, *Collapsing effects in numerical simulation of a class of chaotic dynamical systems and random mappings with a single attracting centre*, Phys. D **86** (1995), no. 4, 559–571. MR 1353178 (96e:58098)

[DM07] Jérôme Dedecker and Florence Merlevède, *The empirical distribution function for dependent variables: asymptotic and nonasymptotic results in* $\mathbb{L}^p$, ESAIM, Probab. Stat. **11** (2007), 102–114.

[DSKP96] Phil Diamond, M. Suzuki, Peter Kloeden, and Alexei Pokrovskii, *Statistical properties of discretizations of a class of chaotic dynamical systems*, Comput. Math. Appl. **31** (1996), no. 11, 83–95. MR 1392078 (96m:58164)

[DV98] Phil Diamond and Igor Vladimirov, *Asymptotic independence and uniform distribution of quantization errors for spatially discretized dynamical systems*, Internat. J. Bifur. Chaos Appl. Sci. Engrg. **8** (1998), no. 7, 1479–1490.

[DV02a] ———, *Branching processes and computational collapse of discretized unimodal mappings*, Internat. J. Bifur. Chaos Appl. Sci. Engrg. **12** (2002), no. 12, 2847–2867.

[DV02b] ———, *Set-valued Markov chains and negative semitrajectories of discretized dynamical systems*, J. Nonlinear Sci. **12** (2002), no. 2, 113–141.

[ERDF83] T. Erber, T. M. Rynne, W. F. Darsow, and M. J. Frank, *The simulation of random processes on digital computers: unavoidable order*, J. Comput. Phys. **49** (1983), no. 3, 394–419.

[Flo02] Paul Philipp Flockermann, *Discretizations of expanding maps*, Ph.D. thesis, ETH (Zurich), 2002.

[GB88] Paweł Góra and Abraham Boyarsky, *Why computers like Lebesgue measure*, Comput. Math. Appl. **16** (1988), no. 4, 321–329.

[GM22] Pierre-Antoine Guihéneuf and Maurizio Monge, *Cramér distance and discretizations of circle expanding maps I: theory*, 2022, arXiv 2206.07991.

[GMNP23] S. Galatolo, M. Monge, I. Nisoli, and F. Poloni, *A general framework for the rigorous computation of invariant densities and the coarse-fine strategy*, Chaos, Solitons & Fractals **170** (2023), 113329.

[GN14] Stefano Galatolo and Isaia Nisoli, *An elementary approach to rigorous approximation of invariant measures*, SIAM Journal on Applied Dynamical Systems **13** (2014), no. 2, 958–985.

[GNR14] Stefano Galatolo, Isaia Nisoli, and Cristóbal Rojas, *Probability, statistics and computation in dynamical systems*, Math. Structures Comput. Sci. **24** (2014), no. 3, e240304, 25.

[GS22] Stefano Galatolo and Alfonso Sorrentino, *Quantitative statistical stability and linear response for irrational rotations and diffeomorphisms of the circle*, Discrete Contin. Dyn. Syst. **42** (2022), no. 2, 815–839.

[Gui15a] Pierre-Antoine Guihéneuf, *Discrétisations spatiales de systèmes dynamiques génériques*, Ph.D. thesis, Université Paris-Sud, 2015.

[Gui15b] ———, *Dynamical properties of spatial discretizations of a generic homeomorphism*, Ergodic Theory Dynam. Systems **35** (2015), no. 5, 1474–1523.

[Gui15c] ———, *Physical measures of discretizations of generic diffeomorphisms*, to appear in Ergodic Theory and Dynamical Systems, arXiv:1510.00720, 2015.

[Gui19] ———, *Degree of recurrence of generic diffeomorphisms*, Discrete Anal. (2019), Paper No. 1, 43.

[KMP99] Peter Kloeden, Jamie Mustard, and Alexei V. Pokrovskii, *Statistical properties of some spatially discretized dynamical systems*, Z. Angew. Math. Phys. **50** (1999), no. 4, 638–660. MR 1709708 (2000e:37039)

[Lan98] Oscar E. Lanford, *Informal remarks on the orbit structure of discrete approximations to chaotic maps*, Experiment. Math. **7** (1998), no. 4, 317–324.

[Lev82] Yves-Emmanuel Levy, *Some remarks about computer studies of dynamical systems*, Phys. Lett. A **88** (1982), no. 1, 1–3.

[Mie05] Tomasz Miernowski, *Dynamique discrétisée et stochastique, géométrie conforme*, Ph.D. thesis, ÉNS de Lyon, 2005.

[Mie06] ———, *Discrétisations des homéomorphismes du cercle*, Ergodic Theory Dynam. Systems **26** (2006), no. 6, 1867–1903.

[MNP15] Maurizio Monge, Isaia Nisoli, and Federico Poloni, *CompInvMeas-Python, Computation of Invariant Measures in Python*, 2015, `https://bitbucket.org/fph/compinvmeas-python/src/master/`.

[Rac91] Svetlozar T. Rachev, *Probability metrics and the stability of stochastic models*, Wiley Series in Probability and Mathematical Statistics: Applied Probability and Statistics, John Wiley & Sons, Ltd., Chichester, 1991.

[SB86] Manuel Scarowsky and Abraham Boyarsky, *Long periodic orbits of the triangle map*, Proc. Amer. Math. Soc. **97** (1986), no. 2, 247–254.

[The22] The Sage Developers, *Sagemath, the Sage Mathematics Software System (Version 9.2)*, 2022, `https://www.sagemath.org`.

[VKD00] Igor Vladimirov, Nikolai Kuznetsov, and Phil Diamond, *Frequency measurability, algebras of quasiperiodic sets and spatial discretizations of smooth dynamical systems*, Math. Comput. Simulation **52** (2000), no. 3-4, 251–272.

[Vla96] Igor Vladimirov, *Quantized linear systems on integer lattices: a frequency-based approach*, CADSEM Reports, Geelong, Australia: Center for Applied Dynamical Systems and Environmental Modeling, Deakin University **96-032, 96-033** (1996), Parts I,II.

[Voe67] Valentin V. Voevodin, *The asymptotic distribution of round-off errors in linear transformations*, Ž. Vyčisl. Mat i Mat. Fiz. **7** (1967), 965–976.

[VV03] Franco Vivaldi and Igor Vladimirov, *Pseudo-randomness of round-off errors in discretized linear maps on the plane*, Internat. J. Bifur. Chaos Appl. Sci. Engrg. **13** (2003), no. 11, 3373–3393.

Pierre-Antoine Guihéneuf: Sorbonne Université and Université de Paris, CNRS, IMJ-PRG, F-75005 Paris, France.

Email address: `pierre-antoine.guiheneuf@imj-prg.fr`

Maurizio Monge: Instituto de Matemàtica da UFRJ, Av. Athos da Silveira Ramos 149, Centro de Tecnologia, Bloco C Cidade Univesitària, Ilha do Fundão, Caixa Postal 68530 21941-909, Rio de Janeiro, RJ, Brasil

Email address: `maurizio.monge@im.ufrj.br`